NACA

RESEARCH MEMORANDUM

AN INVESTIGATION AT LOW SPEED OF A LARGE-SCALE TRIANGULAR

WING OF ASPECT RATIO TWO.- I. CHARACTERISTICS OF A WING

HAVING A DOUBLE-WEDGE AIRFOIL SECTION WITH

MAXIMUM THICKNESS AT 20-PERCENT CHORD

By Adrien E. Anderson

Ames Aeronautical Laboratory
Moffett Field, Calif.

NATIONAL ADVISORY COMMITTEE
FOR AERONAUTICS
WASHINGTON

November 13, 1947

NATIONAL ADVISORY COMMITTEE FOR AERONAUTICS

RESEARCH MEMORANDUM

AN INVESTIGATION AT LOW SPEED OF A LARGE-SCALE TRIANGULAR
WING OF ASPECT RATIO TWO.- I CHARACTERISTICS OF A WING
HAVING A DOUBLE-WEDGE AIRFOIL SECTION WITH
MAXIMUM THICKNESS AT 20-PERCENT CHORD

By Adrien E. Anderson

SUMMARY

An investigation has been made of the low-speed characteristics
of a 25-foot span triangular wing having an aspect ratio of two. The
airfoil section of the wing was a symmetrical double wedge with
5-percent maximum thickness at 20-percent chord. Force and moment
data were obtained at several angles of sideslip for various configu-
rations of 18.5-percent area, constant-chord split flaps, 10-percent-
chord nose flaps, and semispan split-flap-type ailerons. Lift and
drag data were obtained from the plain wing through a limited angle-
of-attack range for Reynolds number varying between 13 and 34 million,
as based on the mean aerodynamic chord.

The results of this investigation show that there are two
regimes of force and moment characteristics exhibited by the wing,
the transition from one to the other being indicated by breaks in
the force and moment curves. These breaks, which occurred at
different values of lift coefficient depending upon the wing
configuration, are believed to indicate an intense separated flow
at the sharp leading edge of the wing.

Below the breaks it was concluded that:

1. Split flaps had moderate lift-producing and trimming
    effectiveness.

2. There was a 12-percent static margin in longitudinal
    stability about the one-quarter mean aerodynamic chord.

3. Dihedral effect and directional stability increased with
    increasing lift.

4. Lateral control remained constant, except in sideslip,
    when the effectiveness of the downstream aileron
    dropped off.

5. The values of rolling and yawing moments varied quite
    uniformly with increasing amounts of either sideslip
    or aileron deflection.

6. Nose flaps were of no benefit as lift devices.

Above the breaks the following characteristics were obtained:

1. Split flaps had low lift-producing effectiveness.

2. There was a reduction in the amount of static margin in
    longitudinal stability.

3. Directional stability, dihedral effect, and lateral control
    dropped off rapidly with increasing lift coefficient.

4. The values of rolling and yawing moments changed rapidly
    with increasing amounts of either sideslip or aileron
    deflection.

5. Any beneficial effects of nose flaps were obtained at the
    sacrifice of other favorable characteristics.

Introduction

    Wings of triangular plan form have become of interest recently,
particularly in the search for wings suitable for high-speed flight.
Until now, however, practically all available aerodynamic information
on wings of triangular plan form has been confined to studies of
small-scale models. In order to obtain data for a large-scale wing
of triangular plan form, having an aspect ratio and maximum thickness
suitable for supersonic flight, an investigation has been conducted
in the Ames 40- by 80-foot wind tunnel. The results of this investi-
gation, which are for a wing of aspect ratio two and a maximum thick-
ness equal to 5-percent of the chord, are reported herein. Although
only a brief analysis of the data has been made at this time, infor-
mation has been provided which will allow an insight into the low-
speed problems of a wing suitable for supersonic flight.

SYMBOLS AND COEFFICIENTS

The standard NACA coefficients and symbols used within this report are defined below and in figure 1:

A aspect ratio $\left(\dfrac{b^2}{S}\right)$

α free-stream angle of attack, degrees

α_{δ_f} rate of change of angle of attack with flap deflection for constant lift coefficient

α_T increment of angle of attack due to wind-tunnel-wall interference, degrees

b wing span, feet

β angle of sideslip, degrees

c wing chord, measured parallel to air stream, feet

$\bar{c}$ mean aerodynamic chord, measured parallel to air stream, feet

C wind-tunnel-test-section area, normal to air stream, square feet

C_L lift coefficient $\left(\dfrac{\text{lift}}{qS}\right)$

C_D drag coefficient $\left(\dfrac{\text{drag}}{qS}\right)$

C_{D_T} increment of drag coefficient due to wind-tunnel-wall interference

C_m pitching-moment coefficient $\left(\dfrac{\text{pitching moment}}{qS\bar{c}}\right)$

C_l rolling-moment coefficient $\left(\dfrac{\text{rolling moment}}{qSb}\right)$

C_Y side-force coefficient $\left(\dfrac{\text{side force}}{qS}\right)$

C_{l_β} rate of change of rolling-moment coefficient with sideslip, per degree

C_{n_β} rate of change of yawing-moment coefficient with sideslip, per degree

$C_{l_{\delta_a}}$ rate of change of rolling-moment coefficient with aileron angle, per degree

$C_{n_{\delta_a}}$ rate of change of yawing-moment coefficient with aileron angle, per degree

δ_a split-flap-type aileron deflection, measured perpendicular to hinge line, degrees

δ_f split-flap deflection, measured perpendicular to hinge line, degrees

δ_w wind-tunnel-wall-interference correction factor

L/D ratio of lift to drag

ν kinematic viscosity, square feet per second

q dynamic pressure, pounds per square foot

R Reynolds number $\left(\dfrac{V\text{c}}{\nu} \right)$

S wing area, square feet

V free-stream velocity, feet per second

EQUIPMENT

The plan form of the wing was that of an isosceles triangle with an apex angle of 53.13°, which made the angle of sweepback of the leading edge 63.43° and the aspect ratio two. The wing had a symmetrical double-wedge airfoil section with a maximum thickness of 5 percent at 20 percent chord. The principal dimensions of the wing are given in figure 2.

The structure of the wing consisted of a plywood skin attached to a steel frame which was built around a boxed-in H-beam, the latter serving as the tail boom. It was necessary to use a tail boom for mounting purposes with the strut arrangement employed.

The hinge line of the split flaps was located parallel to the trailing edge of the wing. The span was terminated at the line of

maximum airfoil—section thickness (86 percent of the wing span),
thus establishing a flap area equal to 18.5 percent of the wing
area. (See fig. 2(b).) These flaps could be attached to either
the upper or lower surface of the wing, were adjustable through a
flap deflection range of 60°, and were divided at the center line
of the wing so that split—flap—type ailerons could be simulated.

The 10—percent—chord nose flaps extended over the same percent
span as the split flaps, and were deflected forward and down to a
fixed angle of 14.5° (measured parallel to the wind stream and with
reference to the projected chord plane of the wing. (See fig. 2(b).)
The leading edge of the nose flap was reinforced with tubing of
varying diameter which formed a nose radius averaging approximately
0.002c at any point.

Figure 3 presents general views of the wing for various
configurations.

TESTS

Force and moment data were obtained through the angle—of—
attack range at various angles of sideslip for the plain wing,
and for the split flap and the split—flap—type—aileron configu-
rations of the wing. In the case of the nose flaps, however, data
were obtained only at zero angle of sideslip. The majority of the
investigation was conducted at dynamic pressures between 15 and 25
pounds per square foot which corresponds to a Reynolds number range
of approximately 11.8×10^6 to 15.4×10^6 as based on the mean
aerodynamic chord. Lift and drag data were obtained for the plain
wing through a limited angle—of—attack range at Reynolds numbers
between 13×10^6 and 34×10^6. Table I contains a summary of the
various configurations tested.

RESULTS

The data are presented about the stability axes with their
origin located at 50 percent of the root chord, which corresponds
to the intersection of the root chord and a line joining the quarter—
chord station of the mean aerodynamic chords.

All the data have been corrected for air—stream inclination and
for wind—tunnel—wall effect, the latter correction being that for a
wing of the same span but with rectangular plan form. The following
corrections, based on the theory of reference 1 for a wind tunnel

with oval cross section, were applied:

$$\alpha_T = \delta_w \ \frac{S}{C} \ C_L \times 57.3 = 0.732 \ C_L$$

$$C_{D_T} = \delta_w \ \frac{S}{C} \ C_L{}^2 = 0.01277 \ C_L{}^2$$

where

$$\delta_w = 0.1167 \text{ and } C = 2356 \text{ square feet}$$

Consideration of the forces acting on the tail boom indicated that its tare effect would be negligible. Drag and pitching-moment tares resulting from strut interference, based on tares obtained with a rectangular wing, were applied to the data.

Table I, the summary of the configurations tested, should also serve as an index for figures 4 to 13 in which the basic data are presented.

The aerodynamic effect of the gap between the two halves of the split flap (fig. 3(b)) was investigated by sealing the gap. The effect, as shown in figure 5 for a flap deflection of 29.5^c, was considered to be negligible; hence, the gap was left unsealed for the other flap deflections.

DISCUSSION

Longitudinal Characteristics

The lift-curve slope through zero lift for the plain wing was 0.040 per degree compared to 0.045 as predicted by lifting surface theory (reference 2) for a wing of aspect ratio two. The theory of reference 3 gives a value of 0.055 per degree; however, this theory is applicable only to wings of very low aspect ratio.

The maximum lift coefficient of 1.36 obtained with the plain wing compares favorably with that obtained on wings of conventional plan form and aspect ratio. However, $C_{L_{max}}$ is obtained at 33° angle of attack, which results in an excessive landing attitude.

The discontinuities which appear in the lift curves shown in figure 4 are believed to be the result of boundary-layer separation around the sharp leading edge of the wing. This type of flow has been

previously discussed in reference 4. The severity of these breaks and the value of C_L at which they occur increased with increasingly positive flap deflection; whereas increasingly negative flap deflections had the opposite effect.

The lift-producing effectiveness of split flaps is usually represented by the parameter α_{δ_f}; however, for this wing the use of α_{δ_f} leads to an erroneous interpretation of flap effectiveness. It appears from the α_{δ_f} curve (fig. 14) that the lift-producing effectiveness is the same (-0.23) above and below the break in the lift curves. (The irregularity shown on the curve is a result of the progressive change in the magnitude of the break and the angle of attack at which it occurs.) Since α_{δ_f} represents, through zero flap deflection, the rate of change of angle of attack of the wing with flap deflection at a given lift coefficient, consideration must be given to the increment of lift due to a given flap deflection at various angles of attack (fig. 15). In the range of angles of attack below the break in the lift curve (represented by $\alpha = 0°$ and 13° in fig. 15) the lift-producing effectiveness holds quite well with increasing flap deflection; whereas beyond the break the rapid reduction in lift-curve slope causes the effectiveness to drop off rapidly (shown by the curves for $\alpha = 19°$ and 24°). For the negative flap-deflection range tested there was little or no change in the almost linear variation of flap effectiveness.

The curve for maximum lift in figure 16 indicates that the largest increment in $C_{L_{max}}$ which could be obtained from the split flaps was 0.04 at an 18° flap deflection. Correspondingly there was a reduction of 2° in the angle of attack for $C_{L_{max}}$. Further increase in flap deflection resulted in a loss in lift, until at 59° flap deflection the value of $C_{L_{max}}$ dropped below that for the plain wing by an increment of 0.08. It is thus apparent that split flaps are of little or no value in increasing $C_{L_{max}}$.

The use of nose flaps resulted in an increase in lift over the plain wing configuration at angles of attack greater than 18°; up to this point there was only a slight reduction in lift.(See fig.6(a).) At maximum lift there was an increase in $C_{L_{max}}$ of 0.25; however, this gain was realized only by going to 5° higher angle of attack (38°).

The use of nose flaps in conjunction with split flaps failed to alter the split-flap effectiveness appreciably as regards to maximum lift; that is the lift curve for 44.5° flap deflection still dropped below the lift curve for 22.0° flap deflection at high angles of

attack. By the use of nose flaps in conjunction with split flaps
deflected 22.0°, a gain of 0.27 in $C_{L_{max}}$ over the plain wing was
realized by increasing the angle of attack from 33° to 34°.

It should be noted that the drag curves of figures 4(b) and
4(c) exhibit breaks corresponding to breaks in the lift curves and
increase in severity with increasingly positive flap-deflection
angles. The minimum drag of the plain wing decreased from 0.0091
at a Reynolds number of 14×10^6 to 0.0080 at 34×10^6, as shown in
figure 7. The lift-drag curves of this figure do not cover a suffi-
cient lift range to determine if there is a change in the drag due
to lift over the Reynolds number range considered.

The maximum lift-drag ratio of 10.1 (fig. 17) was obtained at a
C_L of 0.17, which is well below the C_L range for low-speed flight.
Beyond this point the value of L/D dropped off rapidly to the very
low value of 1.6 at $C_{L_{max}}$. It is noteworthy that the L/D curve for
a 22° flap deflection is coincident with that for the plain wing at
large values of lift coefficient. On the other hand with the flaps
deflected -22.0° as for trim at $C_L = 0.81$ ($\alpha = 22°$), the value of L/D
was 2.3 as compared to a value of 3.4 for the plain wing at the same
C_L. If landings are to be made at conventional values of wing load-
ing and L/D (6 to 7) the curve for the wing with zero flap deflection
indicates the necessity of landing lift coefficients as low as 0.4.
Since, as previously noted, any attempt to trim the airplane will
cause the L/D to drop, it becomes apparent that power will be needed
to maintain a sizeable L/D in landing.

Longitudinal stability about the one-quarter mean aerodynamic
chord point was maintained up to and through the stall except for
the unstable breaks in the moment curves (fig. 4(d)) corresponding
to the breaks in the lift curves. The average value of dC_m/dC_L
between a lift coefficient of 0 and 0.6 was -0.12 which indicates
an aerodynamic center (neglecting drag) location at 37 percent of
the mean aerodynamic chord. The corresponding location on the root
chord is 9 percent ahead of the centroid of area, that is, 58 percent
of the root chord.

Large flap deflections produced a destabilizing effect at lift
coefficients above the break in the curve. For example, dC_m/dC_L
varied from -0.14 at $C_L = 0.4$ to -0.09 at $C_L = 1.0$ with flaps
deflected 22.0°; and from -0.15 to -0.02 over the same C_L range for
flaps deflected 59.0°. The severity of the breaks increased with
increasingly positive flap deflections and reduced with increasingly
negative deflections.

The effectiveness of split flaps as a trim device; that is, when deflected negatively, was relatively unaffected by the breaks in the pitching-moment curves (fig. 18). However, at positive deflections the increment of pitching moment held up quite well for angles of attack below the break in the curve and dropped off rapidly at angles of attack above the break.

Nose flaps (fig. 6(c)) not only caused a reduction in the pitching moment, but produced a greater stability change in going from C_L's below the break in the curve to C_L's above. Note the reduction in the amount of longitudinal stability at low values of C_L and the neutral stability at high C_L's for the plain wing (instability when deflected in conjunction with split flaps.) Also there was little or no reduction of the breaks in the pitching-moment curves when the nose flaps were deflected.

Lateral Characteristics

The lateral characteristics of the triangular wing, as determined from the basic data in figures 8 and 9, are summarized in figure 19. The plain wing had a positive dihedral effect which increased steadily to a maximum value ($C_{l_\beta} = -0.0020$) at a lift coefficient ($C_L = 0.55$) which corresponds approximately to the point at which a change takes place in the type of flow over the wing. Beyond this point there is a gradual reduction in C_{l_β} until at $C_{L_{max}}$ it was approximately one-third the maximum value. Part (b) of the same figure, contains the curve for the wing with split flaps at 44.5°. The general pattern of the curve is the same as for the plain wing. The abrupt reduction near the peak is the result of the break in the C_l against C_L curve for -3.7° sideslip (fig. 9(c)). It is quite possible that this break was due to some asymmetry of the flaps, for there was no corresponding break in the basic curves for the plain wing. Unfortunately no data were obtained at +3.7° sideslip with flaps deflected 44.5° which would permit a verification of the model asymmetry theory.

The C_{l_β} curves are drawn as dashed lines at large values of C_L to indicate that in this region the wing exhibited a nonlinear variation of rolling moment with sideslip. Typical examples are shown in parts (c) and (d) of figure 19 as curves of C_l against β for various values of C_L. In the case of the plain wing the curve for $C_L = 0.10$ is approximately linear up to 16° of sideslip, while the curves representing $C_L = 1.02$ exhibits a sudden reversal in slope

beyond 8° of sideslip. Somewhat similar conditions existed for the wing with flaps deflected 44.5°. Hence, the C_{l_β} curves should be considered as indicative of the condition existing at $\pm 4^\circ$ of sideslip.

Split-flap-type aileron effectiveness is summarized in figure 20 from the data in figures 10, 12, and 13. (Note that only one aileron was deflected at a time.) Aileron effectiveness at zero sideslip ($C_{l_{\delta_a}} = 0.00080$) remained constant up to approximately the lift coefficient ($C_L = 0.60$) at which there was a change in the type of flow over the wing, and then dropped to only one-half the original value at $C_{L_{max}}$. At 11.9° sideslip the left or trailing aileron indicated more effectiveness than the right one at low values of C_L but its effectiveness dropped off rapidly until at a C_L of 0.8 it was less effective than the right one. The $C_{l_{\delta_a}}$ curves have been terminated at a C_L of 0.8, since beyond this value the curves of rolling-moment coefficient against aileron deflection show extreme variations from linearity. In part (b) of figure 20, it is shown that regardless of the value of C_L there is a reasonably linear variation of C_l with δ_a at zero sideslip, while in parts (c) and (d) for 11.9° sideslip, there is pronounced nonlinearity at large values of C_L. It is obvious that taking the slope of these curves through $\delta_a = 0$ would only lead to an erroneous interpretation of aileron effectiveness.

Directional Characteristics

The plain wing exhibited increasing directional stability ($dC_{n_\beta}/dC_L \approx 0.0010$) up to a $C_L = 1.05$ with and without flaps deflected (fig. 21, a summary of figs. 8 and 9). Beyond this point the directional stability decreased rapidly to zero at the stall. It is of interest to note that the directional stability did not drop off when the flow over the wing changed at a lower lift coefficient. However, above $C_L = 0.8$ there is a pronounced nonlinear variation of C_n with β, particularly for angles of sideslip greater than 8° as shown in figures 21(c) and 21(d). The C_{n_β} curve is shown as a dashed line in this region. The slight dip in the curve at a $C_L = 0.85$, for the flaps-deflected condition, corresponds to the break in the corresponding C_{l_β} curve of figure 19.

The deflection of a single aileron produced an adverse yawing moment which varied almost linearly ($dC_{n_{\delta_a}}/dC_L \approx -0.00033$) with increasing C_L for the two angles of sideslip considered: 0° and 11.9°. (See fig. 22 for a summary of figs. 10, 12, and 13.)

Particularly noteworthy is the fact that when the wing was at high
angles of attack and 11.9° sideslip the ailerons exhibited different
yawing-moment characteristics, depending upon which direction they
were deflected. (See examples in parts (c) and (d) of fig. 22.)
Under such circumstances the value of $C_{n_{\delta_a}}$ becomes insignificant,
since $C_{n_{\delta_a}}$ is the rate of change of C_n with δ_a through $\delta_a = 0$.
For this reason the curves of $C_{n_{\delta_a}}$ have been terminated at a
C_L of 0.8.

CONCLUDING REMARKS

It appears from the results of this investigation that there are
two types of flow over the wing, typified by smooth flow at low lift
coefficients and by separation off the sharp leading edge at high
lift coefficients. The transition from one type of flow to the other
was indicated by breaks in the force and moment curves. These breaks,
which occurred at different values of lift coefficients, depending
upon the wing configuration, indicate the division between two
generally different regimes of wing characteristics.

The maximum lift coefficient of 1.36, obtained at an angle of
attack of 33°, for the plain wing was increased to only 1.40 by the
use of 18.5-percent-area split flaps deflected 18°. Flap deflections
greater than 18° resulted in a reduction in $C_{L_{max}}$ until at 59.0° the
$C_{L_{max}}$ was less than that of the plain wing by 0.08. The use of 10-
percent-chord nose flaps deflected 14.5° produced a maximum lift
increment of 0.20 for the plain wing, but increased the angle of
attack for maximum lift to 38°. The wing has longitudinal stability
about the one-quarter mean aerodynamic chord point (average
$\frac{dC_m}{dC_L} = -0.12$ for the plain wing) up to and through the stall except
for the unstable breaks in the moment curves near 0.7 lift coefficient
and except for very large flap deflections, which indicated a strong
destabilizing effect at lift coefficients above the break. The wing
exhibited positive dihedral effect and directional stability in side-
slip $\left(\frac{dC_{l_\beta}}{dC_L} = -0.0036; \frac{dC_{n_\beta}}{dC_L} \approx 0.0010, \text{ for the plain wing} \right)$ but the
values of rolling and yawing moment changed abruptly at large angles
of attack in sideslip. Aileron effectiveness ($C_{l_{\delta_a}} = 0.00080$) was

maintained up to a C_L of 0.6 and decreased only slightly thereafter. The rate of change of adverse yawing moment with aileron deflection increased almost linearly with lift coefficient $\left(\frac{dC_{n\delta a}}{dC_L} \approx -0.00033 \right)$; however this parameter was greatly influenced by the direction of the aileron deflection at large values of lift in sideslip.

Ames Aeronautical Laboratory,
    National Advisory Committee for Aeronautics,
        Moffett Field, Calif.

REFERENCES

1. Tani, Itiro, and Sanuki, Matao: The Wall Interference of a Wing Tunnel of Elliptic Cross Section. NACA TM No. 1075, 1944.

2. Krienes, Klaus: The Elliptic Wing Based on the Potential Theory. NACA TM No. 971, 1941.

3. Jones, Robert T.: Properties of Low-Aspect-Ratio Pointed Wings at Speeds Below and Above the Speed of Sound. NACA TN No. 1032, 1946.

4. Wilson, Herbert A., Jr., and Lovell, J. Calvin: Full-Scale Investigation of the Maximum Lift and Flow Characteristics of an Airplane Having Approximately Triangular Plan Form. NACA RM No. L6K20, Feb. 1947.

TABLE I.— SUMMARY OF CONFIGURATIONS INVESTIGATED

Fig-ure	Angle of Sideslip	Wing Configuration			Reynolds Number	Data Presented
		Split Flap	Nose Flap	Aileron		
4	0.0°	-22.0° -16.5° -11.0° -6.0° 0.0° 5.5° 11.0° 17.0° 22.0° 29.5° 44.5° 59.0°	– – –	– – – –	11.8×10^6 and 15.4×10^6	C_L vs $\begin{cases} \alpha \\ C_D \\ C_m \end{cases}$
5	0.0°	29.5° Gap No Gap	– – –	– – – –	15.4×10^6	– – – –
6	0.0°	0.0° 22.0° 44.5°	14.5°	– – – –	13.8×10^6	– – – –
7	0.0°	0.0°	– – –	– – – –	13.3 to 32.2×10^6	C_L vs C_D C_{D_O} vs R
8	-3.7° 0.0° 4.2° 7.9° 11.9° 16.0°	0.0°	– – –	– – – –		
9	-3.7° 0.0° 7.9° 11.9°	44.5°	– – –	– – – –	15.4×10^6	C_L vs $\begin{cases} \alpha \\ C_D \\ C_m \\ C_l \\ C_n \\ C_Y \end{cases}$
10	0.0°	– – –	– – –	Right $-22.0^{\circ}; -11.0^{\circ}$ $0.0^{\circ}; 11.0^{\circ}$		
11	4.2°	– – –	– – –	Right $0.0^{\circ}; 11.0^{\circ}$		
12	11.9°	– – –	– – –	Right, -22.0° $-11.0^{\circ}; 0.0^{\circ};$ $11.0^{\circ}; 22.0^{\circ}$		
13	11.9°	– – –	– – –	Left, $-22.0^{\circ};$ $-11.0^{\circ}; 0.0^{\circ}$ $11.0^{\circ}; 22.0^{\circ}$		
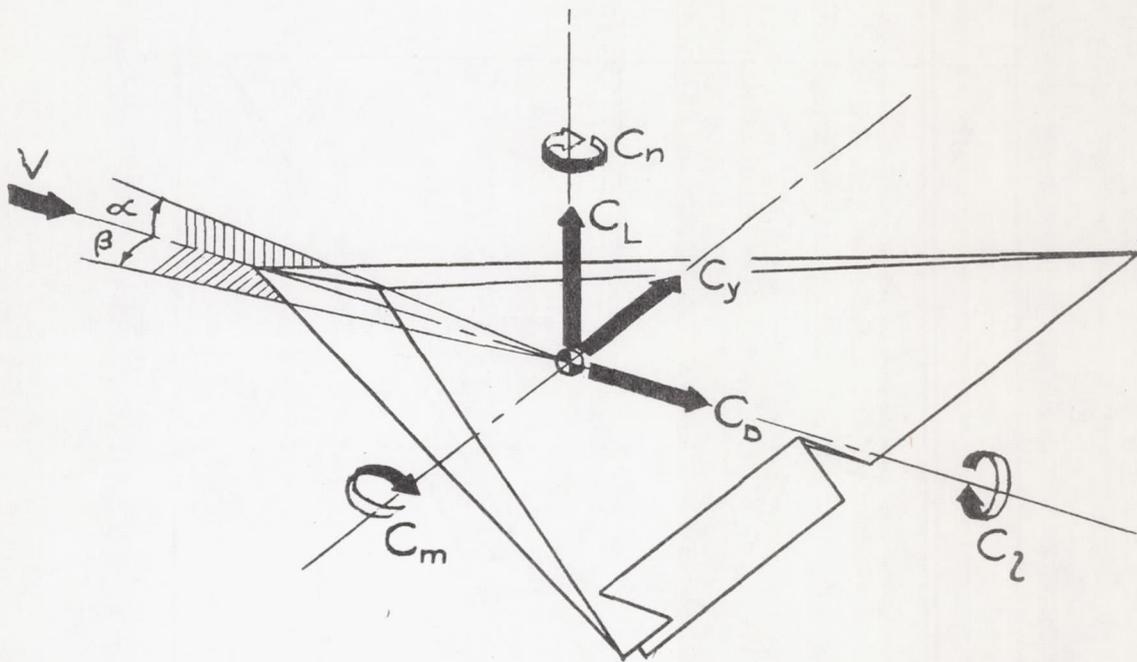
FIGURE 1. – SIGN CONVENTION FOR THE STANDARD NACA COEFFICIENTS. ALL FORCES, MOMENTS, ANGLES, AND CONTROL SURFACE DEFLECTION ARE SHOWN AS POSITIVE.

Fig. 2 a   NACA RM No. A-7F06

.50'

TAIL BOOM

7.00'

M.A.C. = 16.67'

10.00'

MOMENT CENTER 0.25 M.A.C.

25.00'

53.13°

12.50'

WING AREA, S = 312.5 FT.²

5.00'

63.43°

NATIONAL ADVISORY
COMMITTEE FOR AERONAUTICS

25.00'

.50'

1.25'
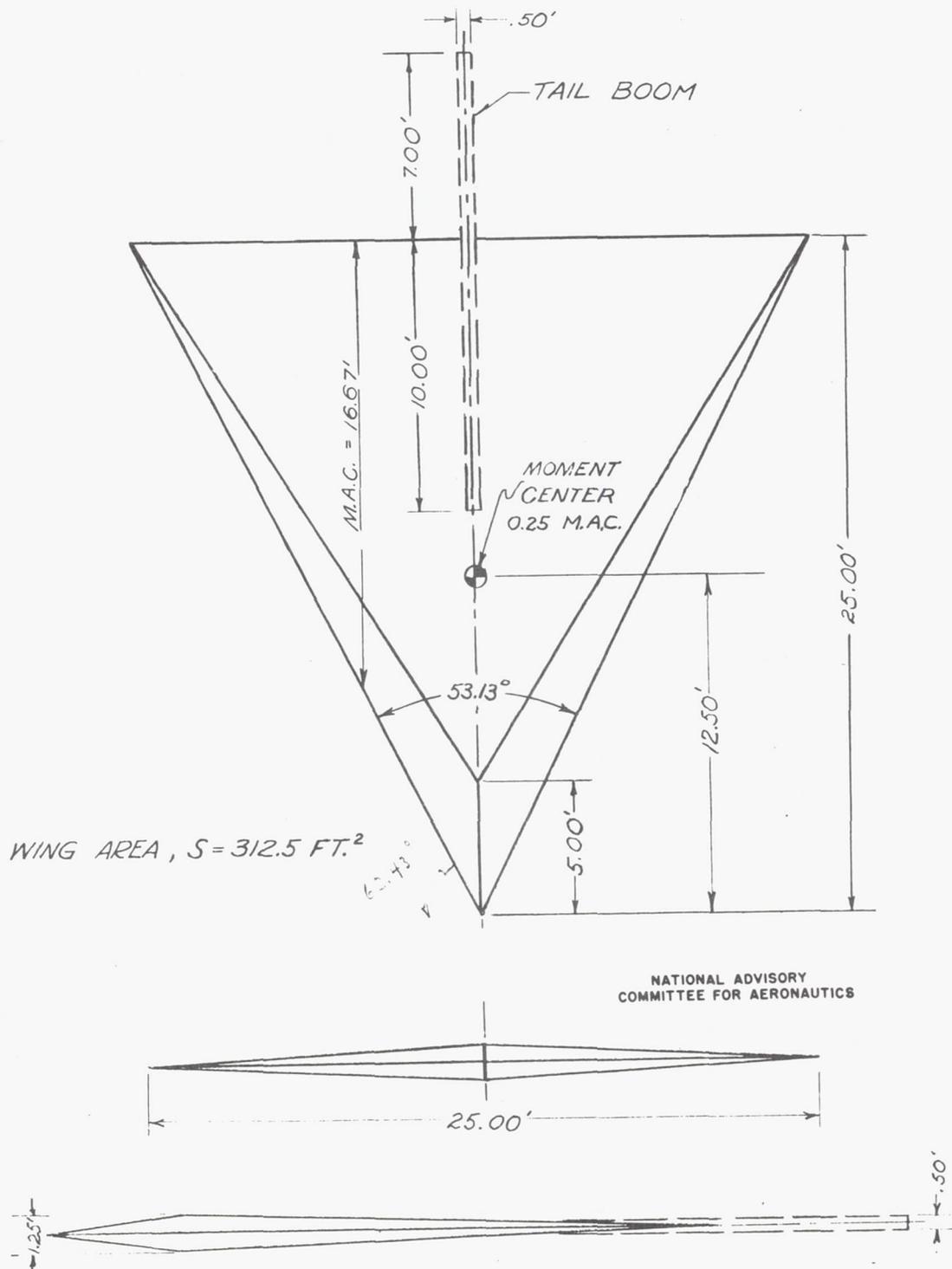
(a.) BASIC WING

FIGURE 2.- GENERAL ARRANGEMENT OF THE LOW
ASPECT RATIO WING WITH TRIANGULAR PLAN FORM.

SPLIT FLAP AREA = .185 S

10.67'

NOSE FLAP AREA = .098 S

10.67'

NATIONAL ADVISORY
COMMITTEE FOR AERONAUTICS

.10 C

δ_f

ROUND TUBING DIAM. = .0040 C.

2.67'

δ_f

SECTION   A-A

SECTION   B-B
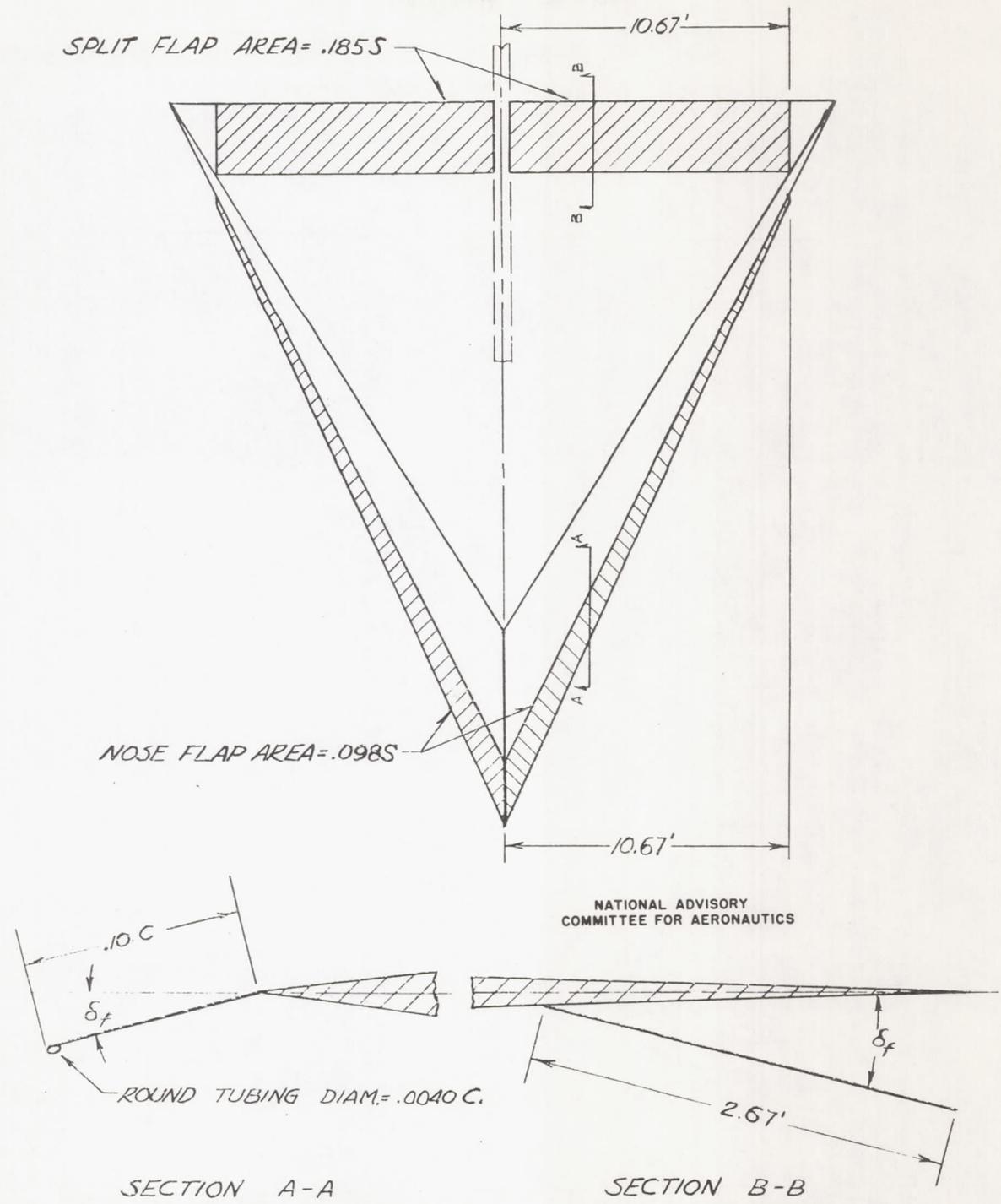
(b) SPLIT FLAPS AND NOSE FLAPS

FIGURE 2.- CONCLUDED
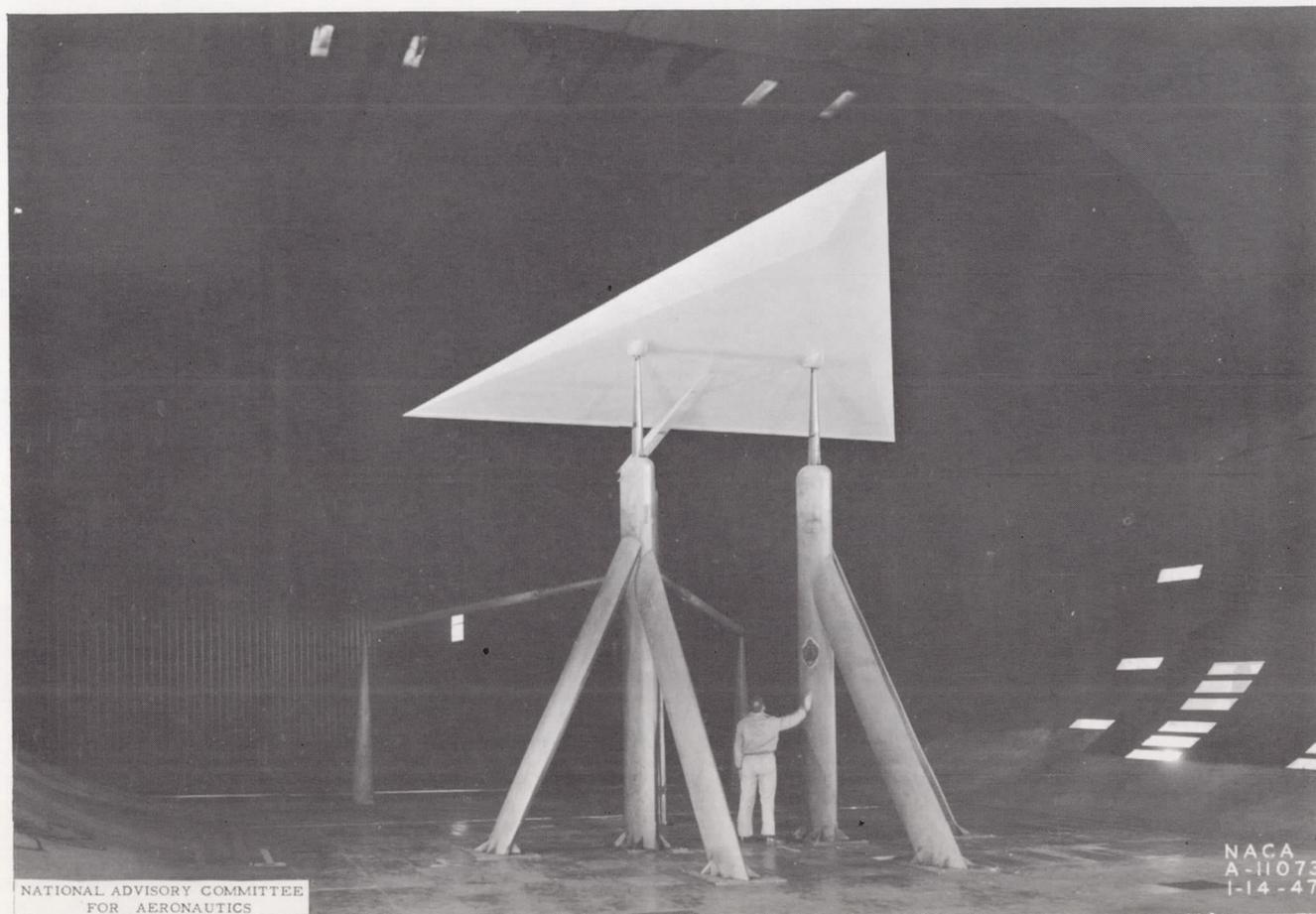
(a) Basic wing.

Figure 3.— The low-aspect-ratio wing with triangular plan form mounted in the Ames 40- by 80-foot
wind tunnel.
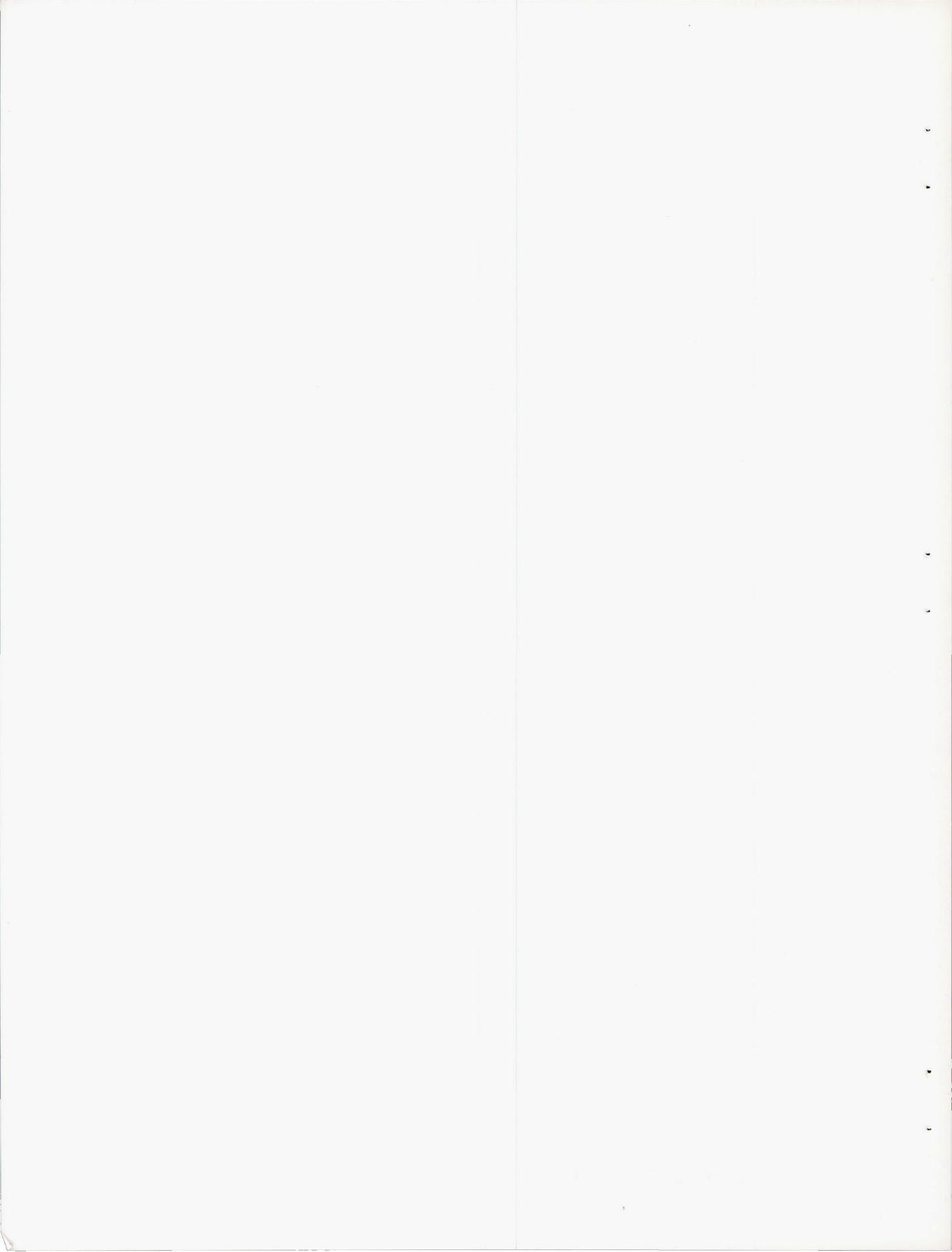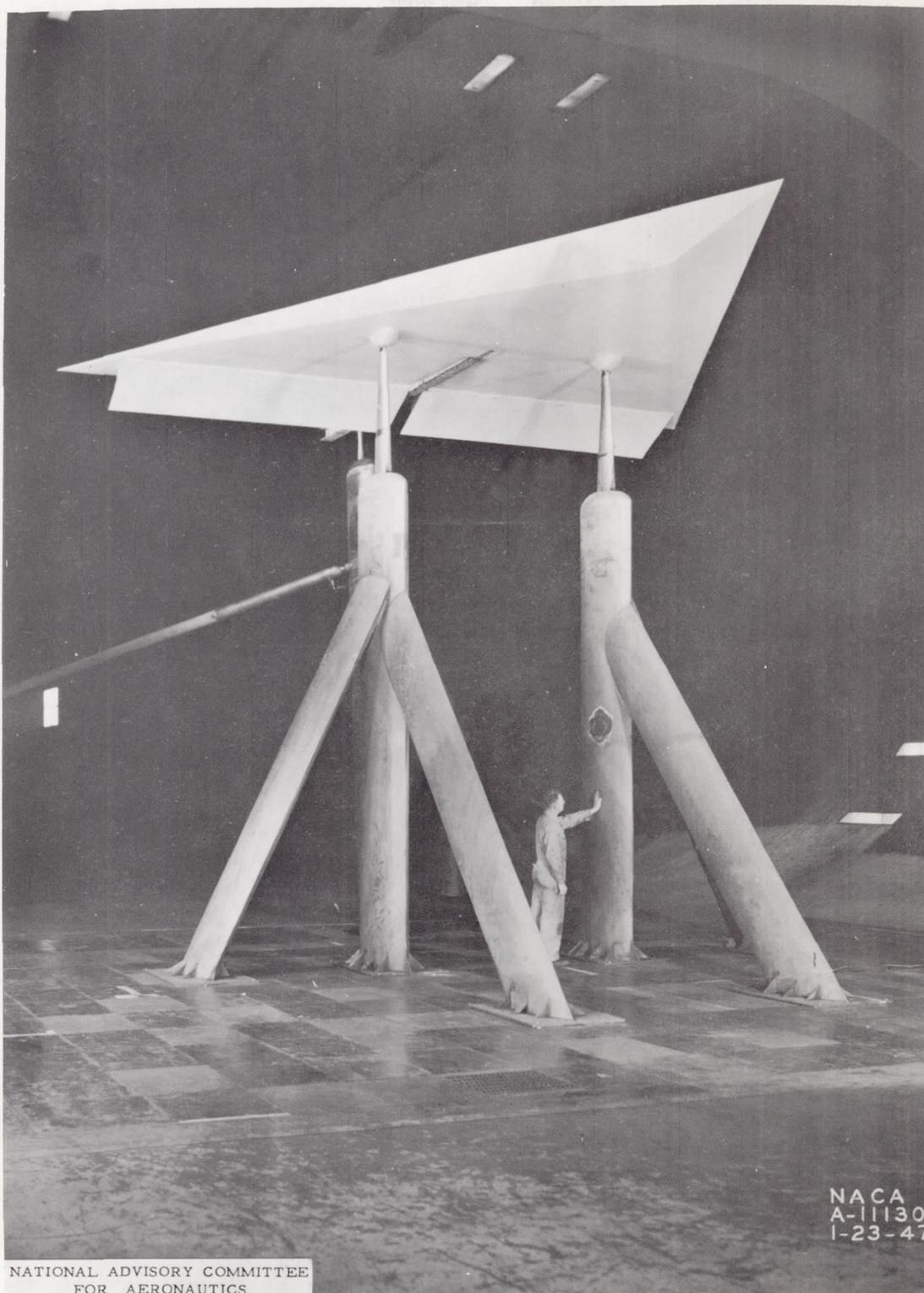
(b) Split flaps at 29.5°.

Figure 3.— Continued.
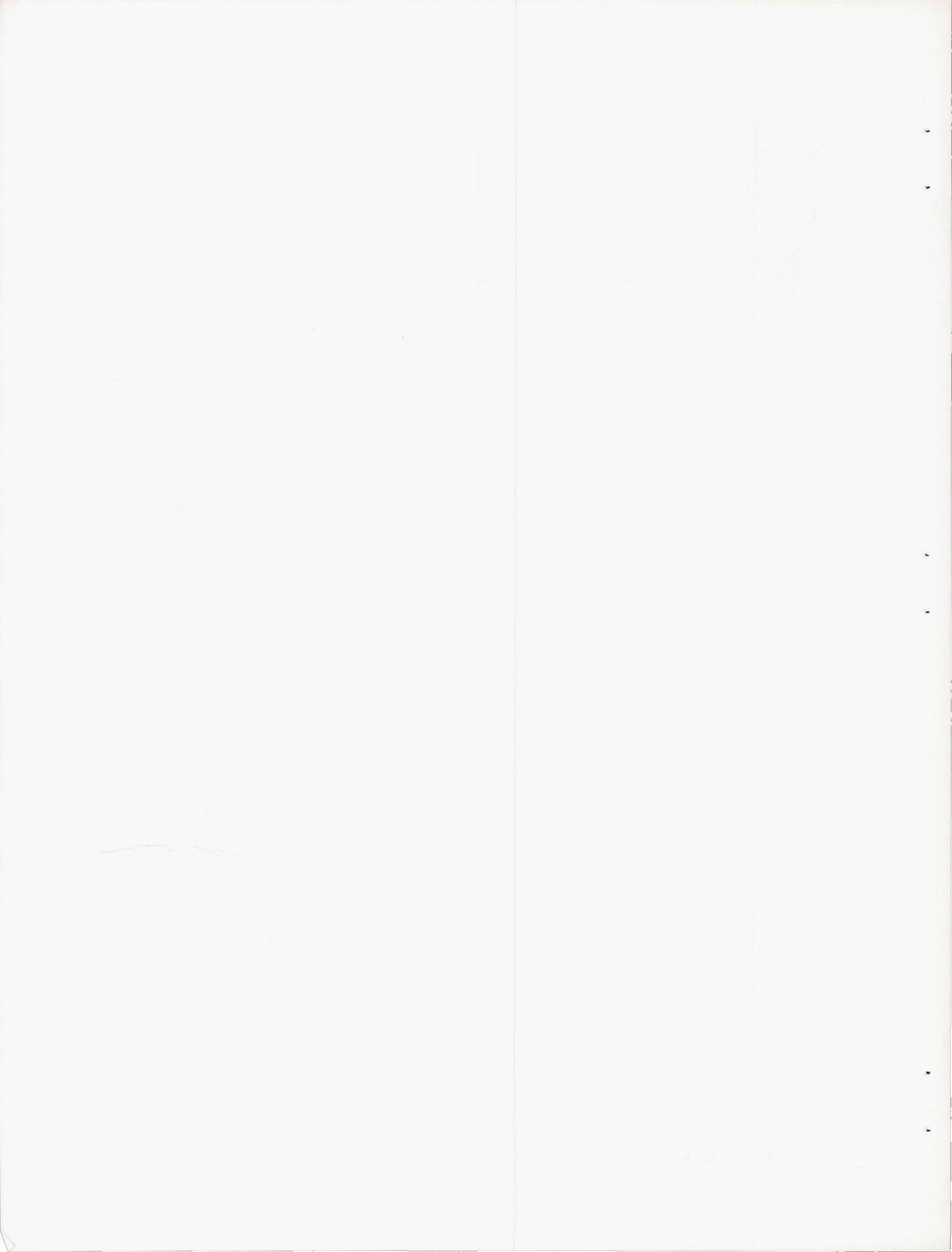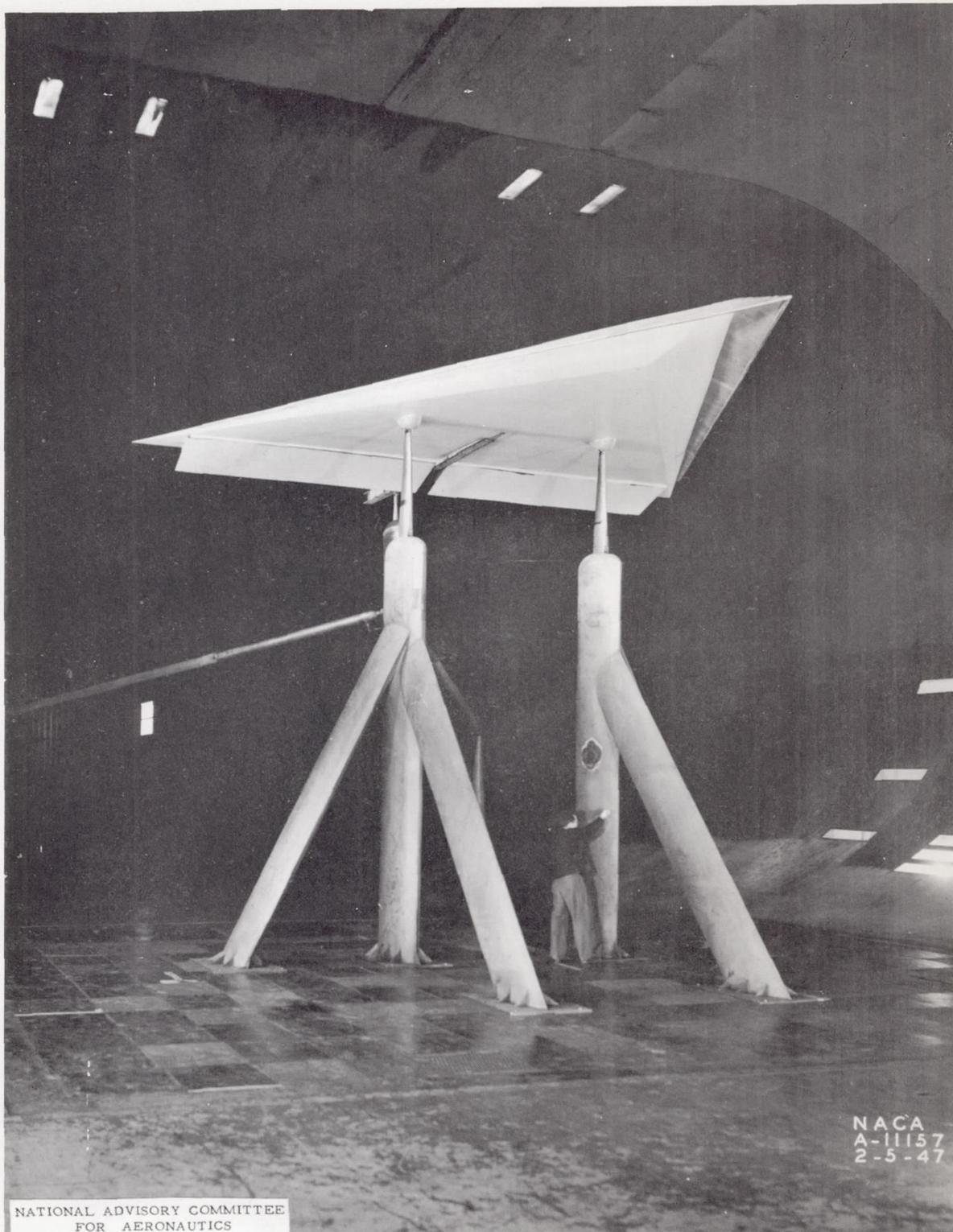
(c) Nose flaps at 15° plus split flaps at 22°.

Figure 3.- Concluded.
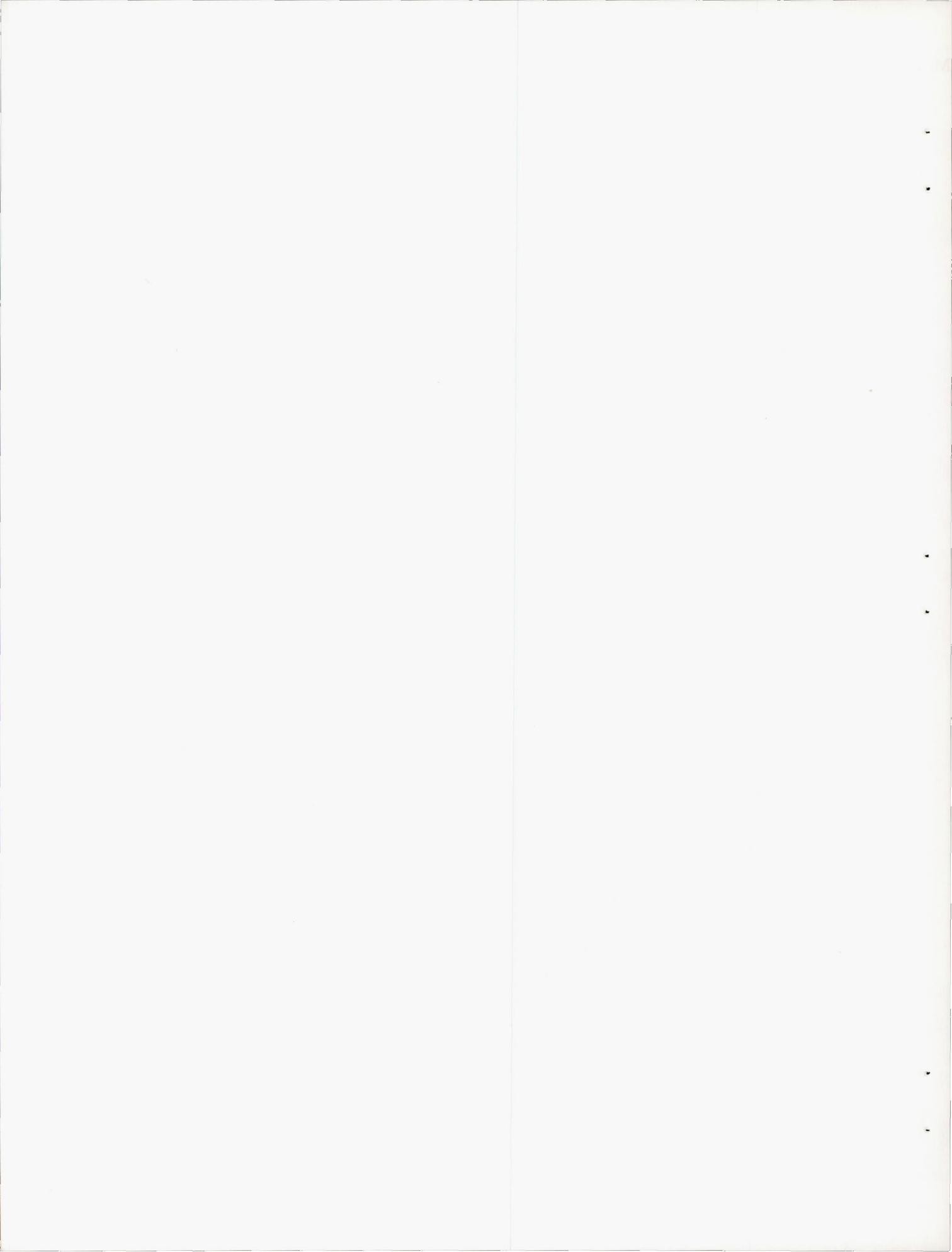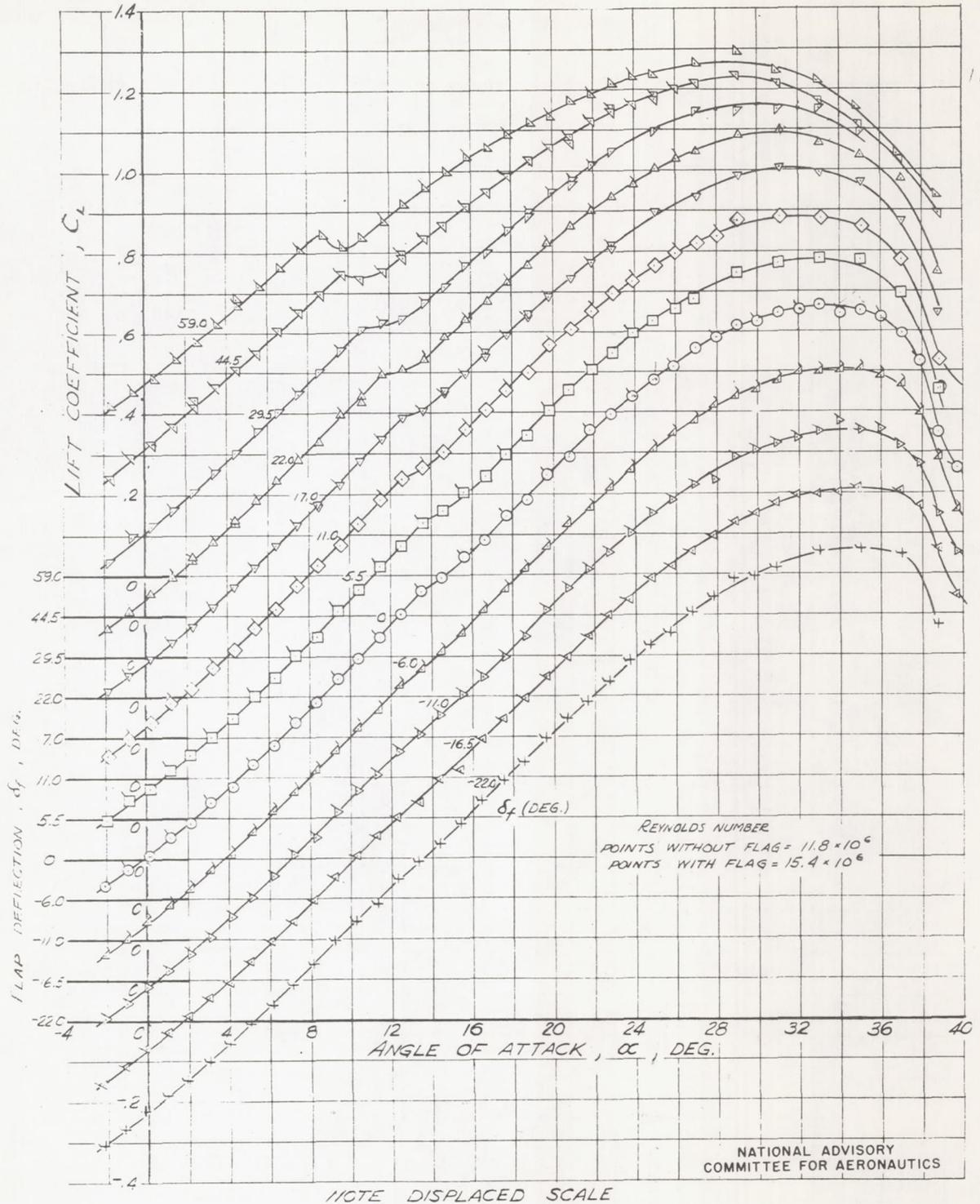
(a) C_L vs α

FIGURE 4 – AERODYNAMIC CHARACTERISTICS OF THE TRIANGULAR WING
WITH 8.5 PERCENT AREA SPLIT FLAPS DEFLECTED -22.0° TO 59.0°.

Fig. 4 b

1.6

1.4

1.2

1.0

.8

.6

.4

.2

0

-.2

LIFT COEFFICIENT, C_L

REYNOLDS NUMBER
POINTS WITHOUT FLAG = 11.8×10^6
POINTS WITH FLAG = 15.4×10^6

59.0 δ_f (DEG)

44.5

29.5

22.0

17.0

11.0

5.5

0

.1   .2   .3   .4   .5   .6   .7   .8   .9   1.0   1.1

DRAG COEFFICIENT, C_D

NATIONAL ADVISORY
COMMITTEE FOR AERONAUTICS
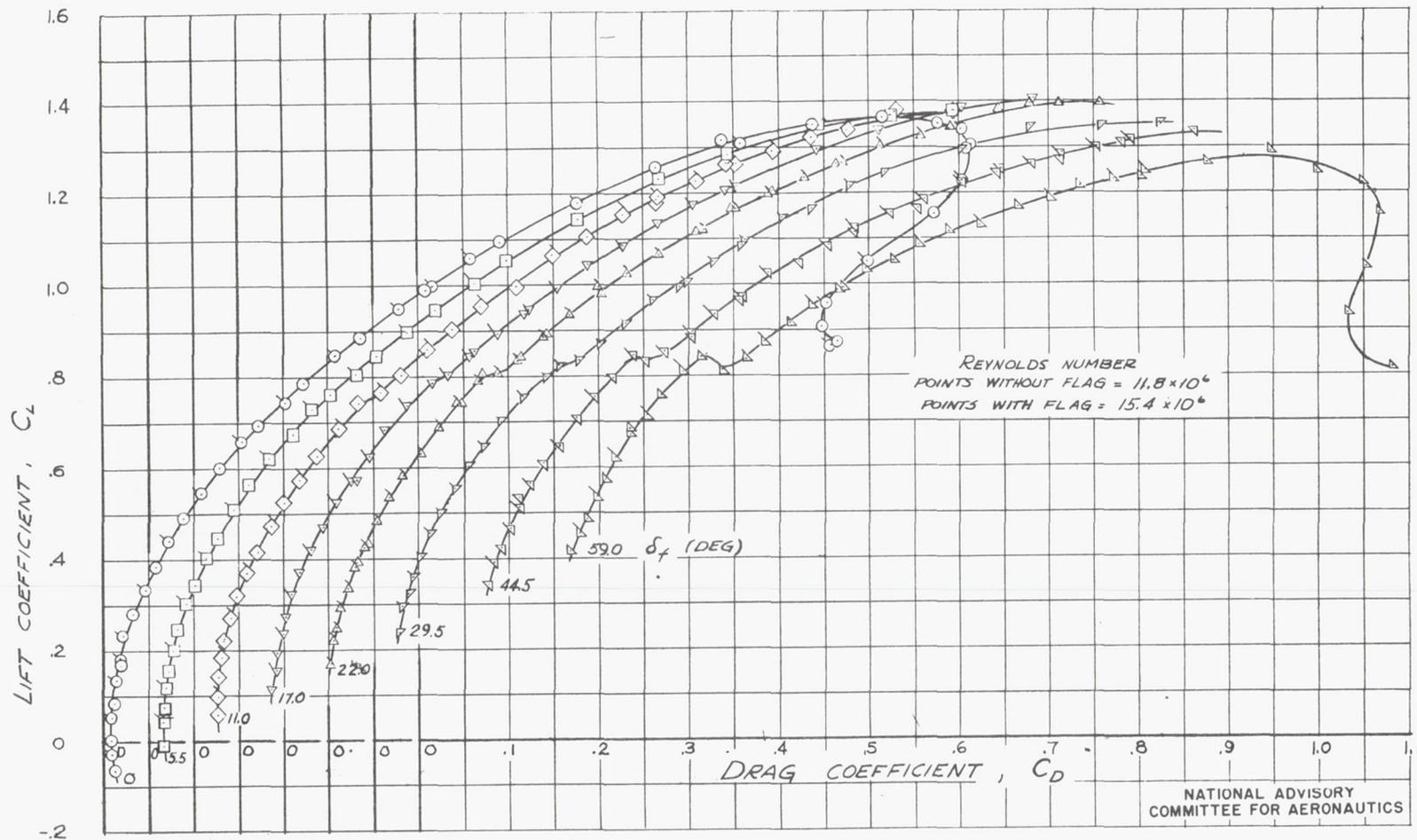
⊙   ⊡   ◇   ▽   △   ▽   ◁   ▷
0   5.5   11.0   17.0   22.0   29.5   44.5   59.0

FLAP DEFLECTION, δ_f, DEG.

(b) C_L vs C_D ($\delta_f = 0°$ to $59.0°$)

FIGURE 4.- CONTINUED.

REYNOLDS NUMBER
POINTS WITHOUT FLAG = 11.8 × 10⁶
POINTS WITH FLAG = 15.4 × 10⁶

NATIONAL ADVISORY
COMMITTEE FOR AERONAUTICS

⊙   △   ▷   ◁   +
0   -6.0   -11.0   -16.5   -22.0
FLAP DEFLECTION , δ_f , DEG.
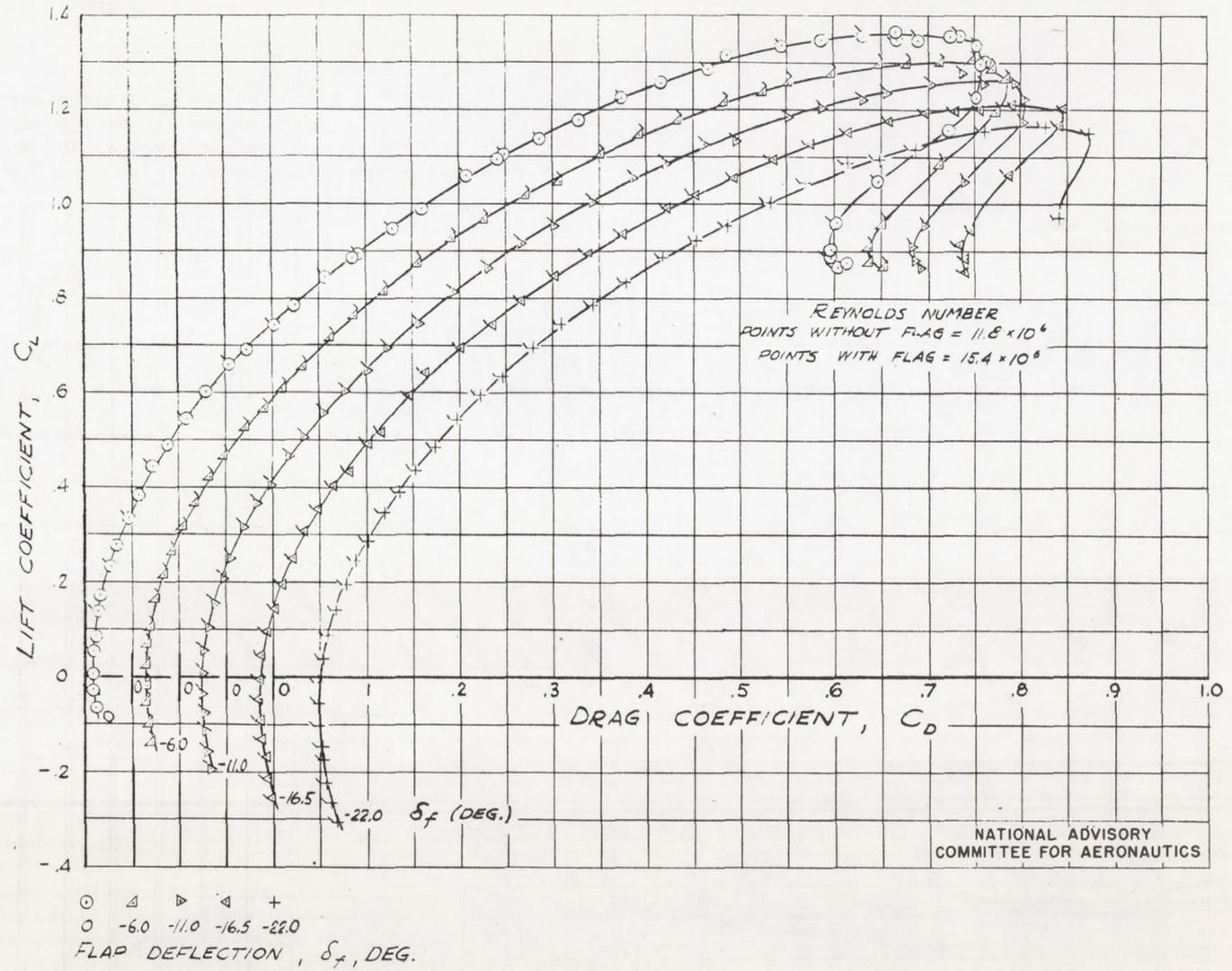
(c) C_L vs C_D $(\delta_f = 0°$ to $-22.0°)$

FIGURE 4.- CONTINUED.

Fig. 4 c
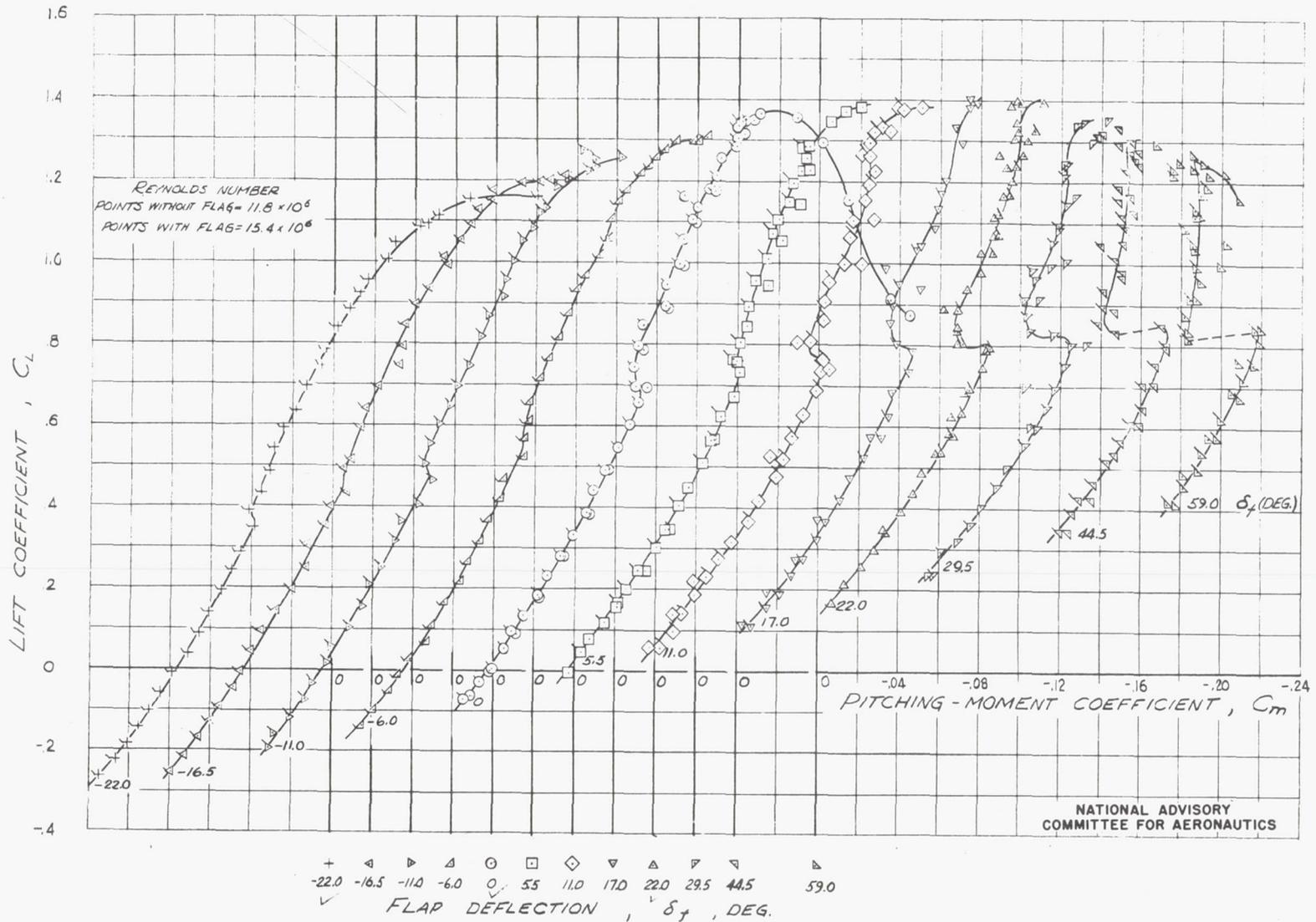
(d) C_L vs C_m

FIGURE 4.- CONCLUDED.

Fig. 4 d
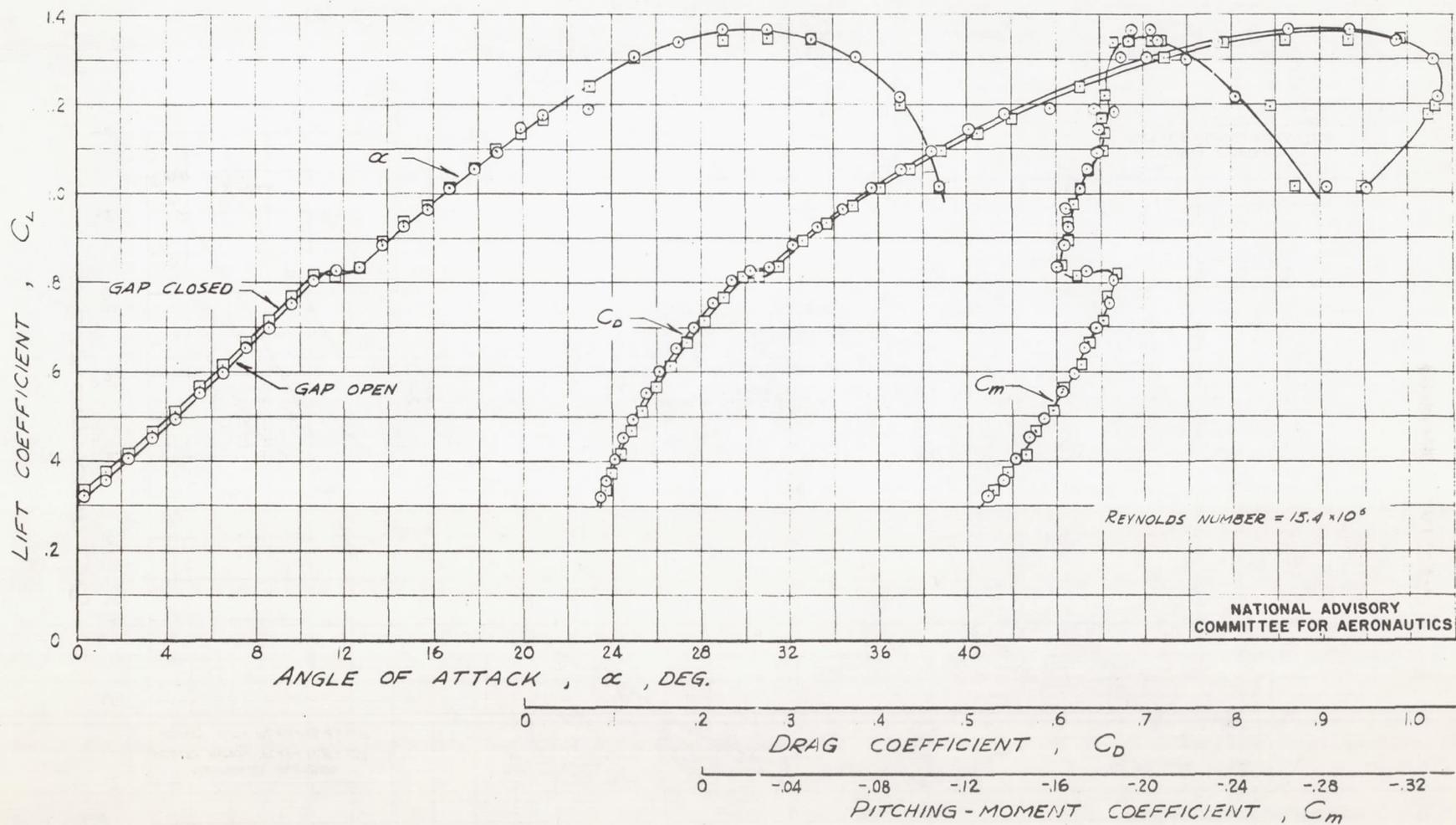
FIGURE 5.- THE EFFECT OF THE SPANWISE GAP IN THE FLAPS ON THE AERODYNAMIC CHARACTERISTICS OF THE TRIANGULAR WING WITH SPLIT FLAPS DEFLECTED 29.5°.

Fig. 5

Fig. 6 a

CONFIGURATION
NOSE FLAPS + δ_f = 22.0°
NOSE FLAPS
NOSE FLAPS + δ_f = 44.5°
PLAIN WING
δ_f = 22.0°
δ_f = 44.5°

} CURVES FROM FIG. 4

REYNOLDS NUMBER = 13.8 × 10⁶

NATIONAL ADVISORY
COMMITTEE FOR AERONAUTICS
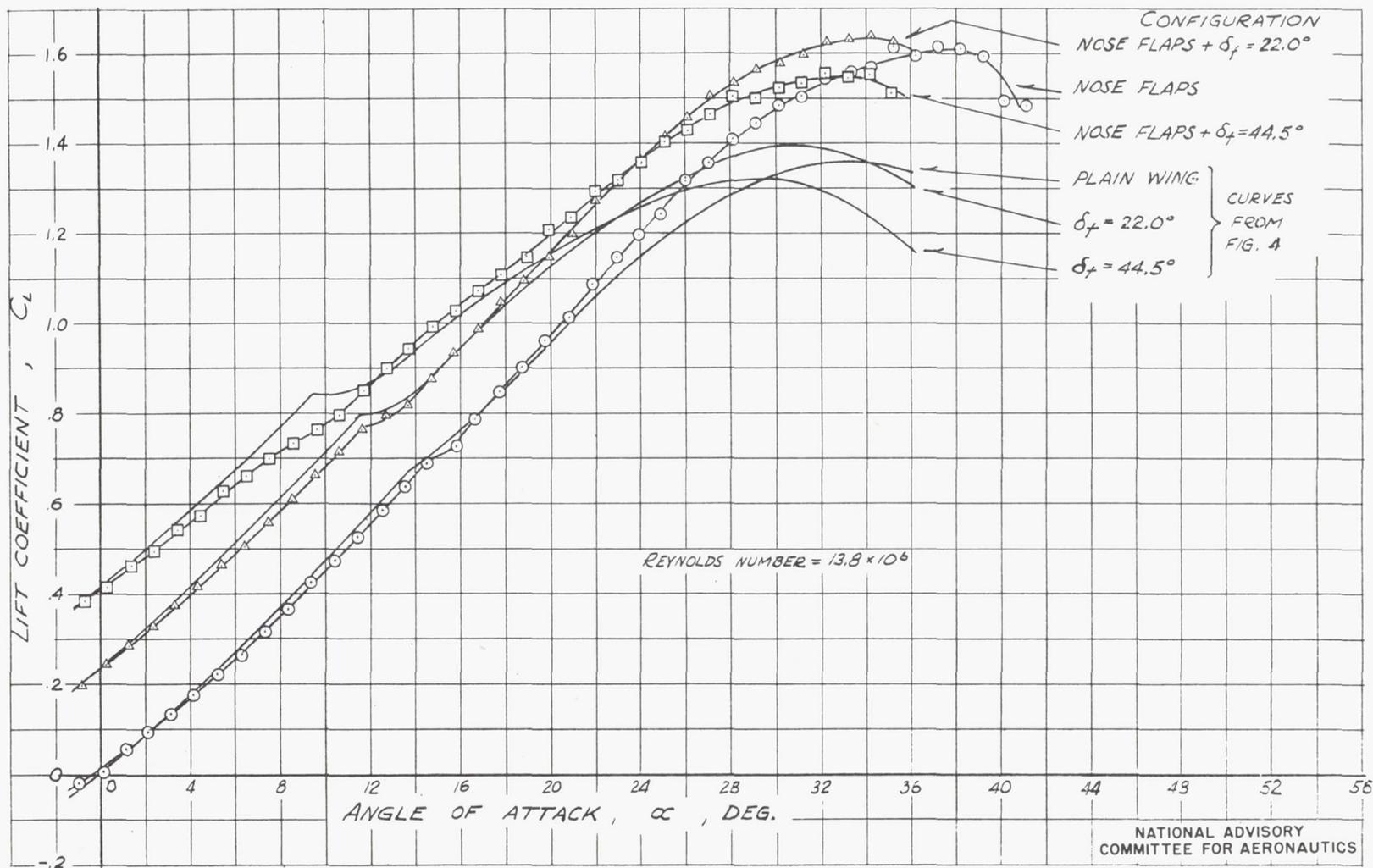
(a) C_L VS α

FIGURE 6.- AERODYNAMIC CHARACTERISTICS OF THE TRIANGULAR WING
WITH 10 PERCENT CHORD NOSE FLAPS DEFLECTED 14.5°.

CONFIGURATION

NOSE FLAP + $\delta_f = 44.5°$

NOSE FLAP

NOSE FLAP + $\delta_f = 22.0°$

PLAIN WING

$\delta_f = 44.5°$

$\delta_f = 22.0°$

CURVES FROM FIG. 4

NATIONAL ADVISORY
COMMITTEE FOR AERONAUTICS
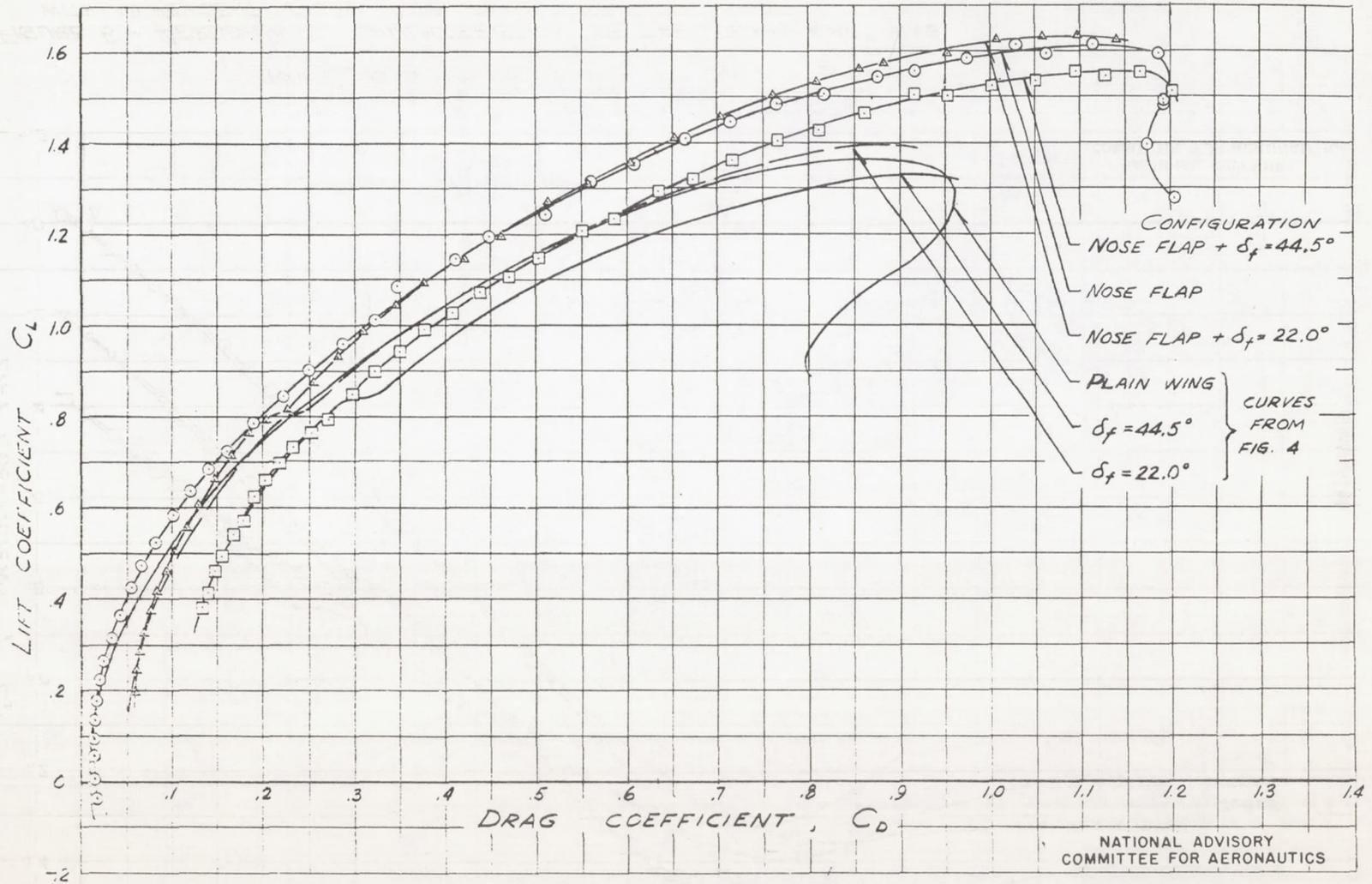
(b) C_L vs C_D

FIGURE 6.- CONTINUED.

Fig. 6 b

Fig. 6 c   NACA RM No. A-7F06
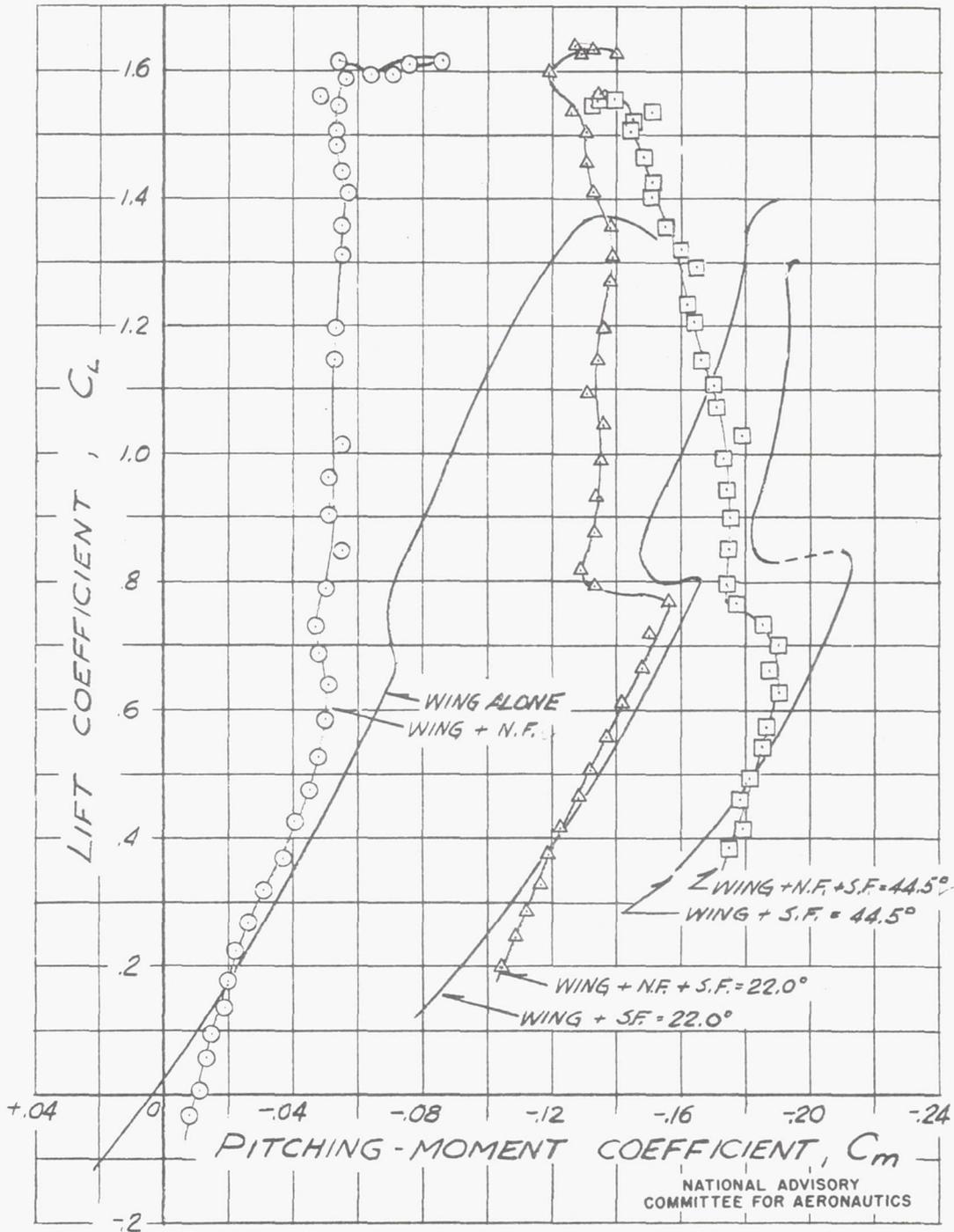
(c) C_L vs C_m

FIGURE 6.- CONCLUDED
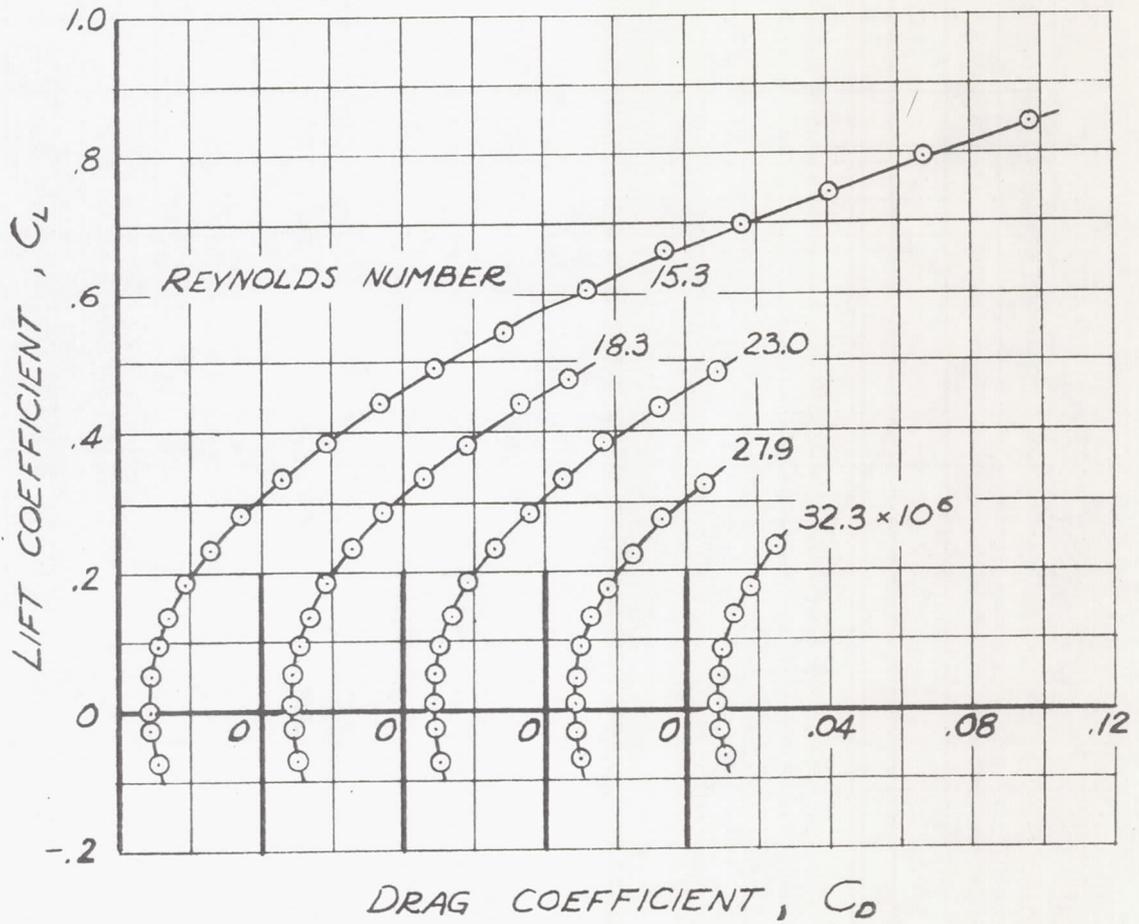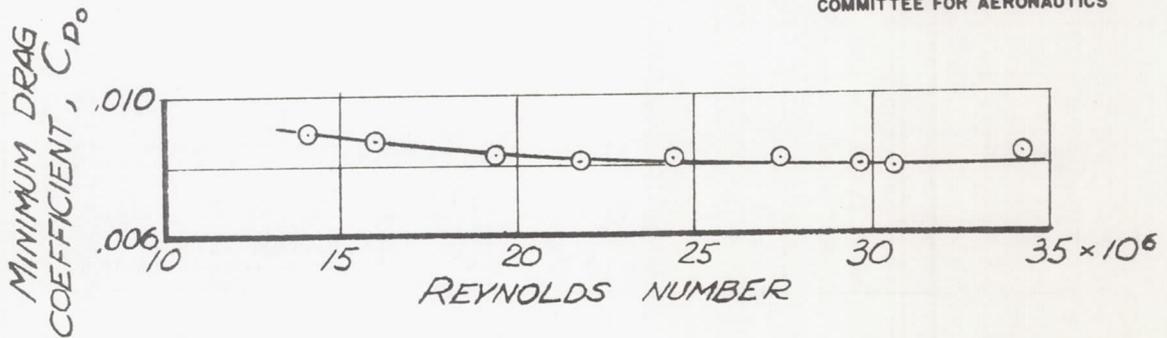
FIGURE 7. — EFFECT OF REYNOLDS NUMBER ON THE DRAG CHARACTERISTICS OF THE PLAIN WING.

Fig. 8 a
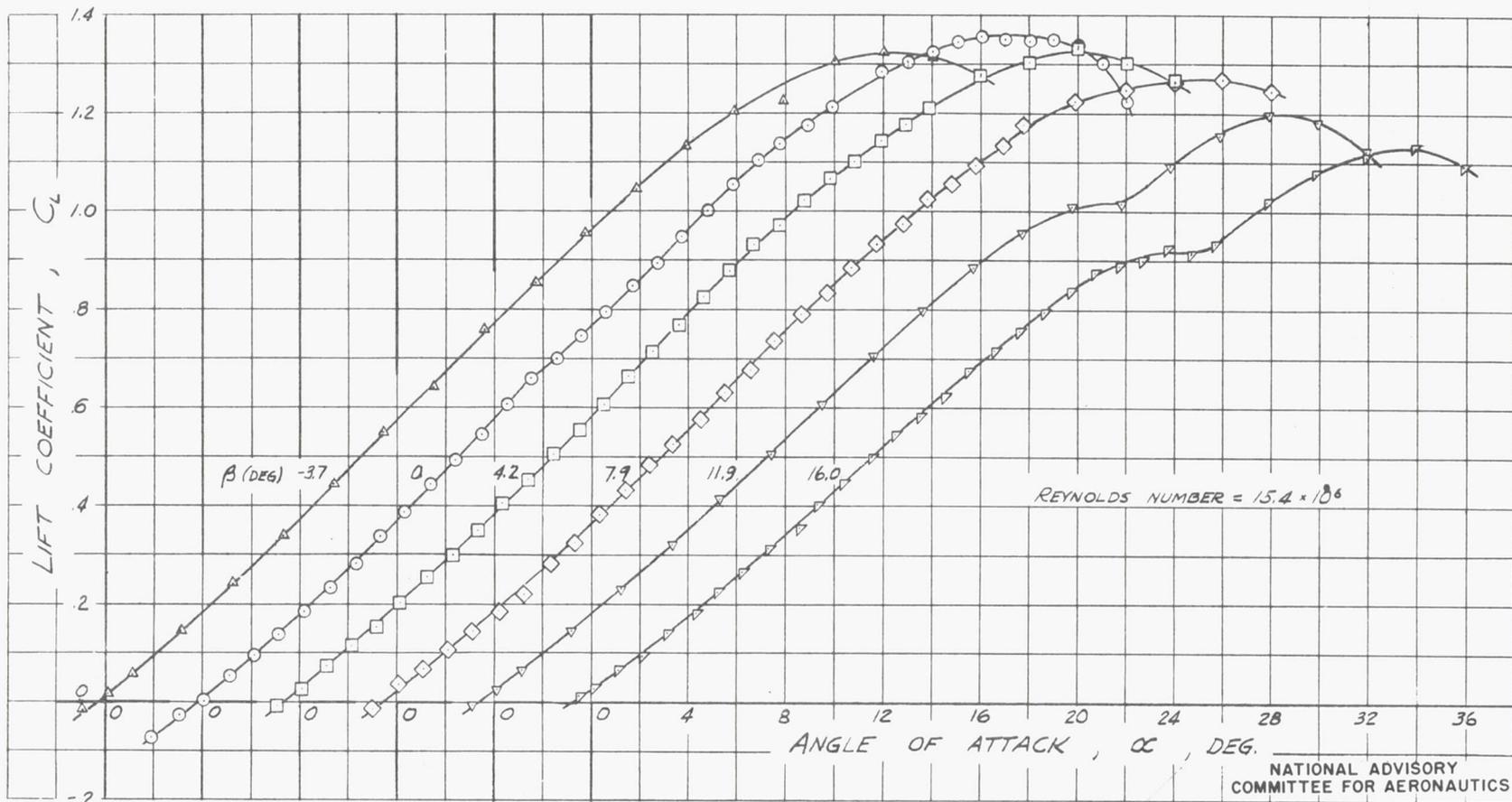
ANGLE OF SIDESLIP , β , DEG.

NOTE DISPLACED SCALES

(a) C_L vs α

FIGURE 8.- AERODYNAMIC CHARACTERISTICS OF THE PLAIN TRIANGULAR
WING AT ANGLES OF SIDESLIP FROM -3.7° TO +16.0°.

Fig. 8 b

(b) C_L VS C_D
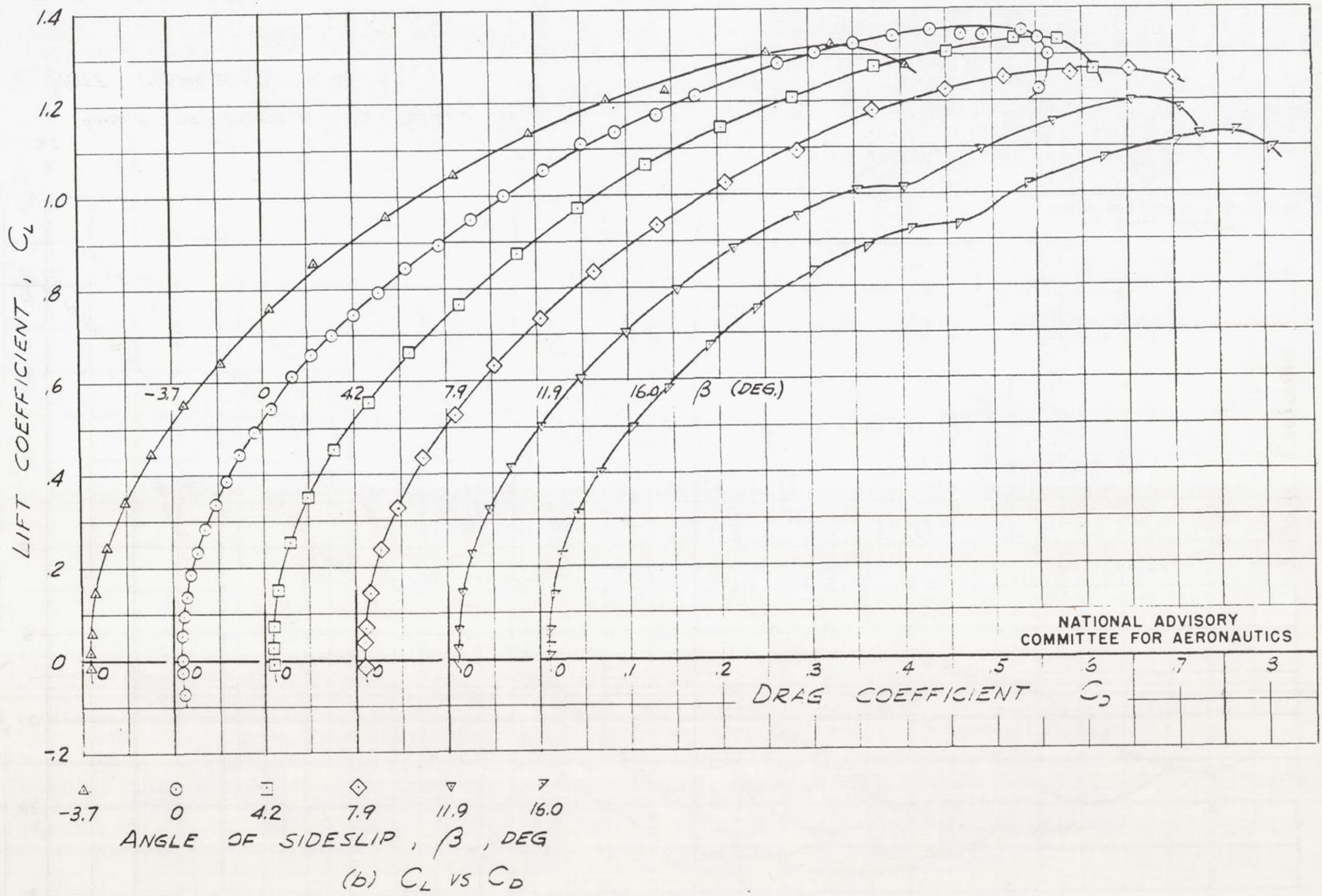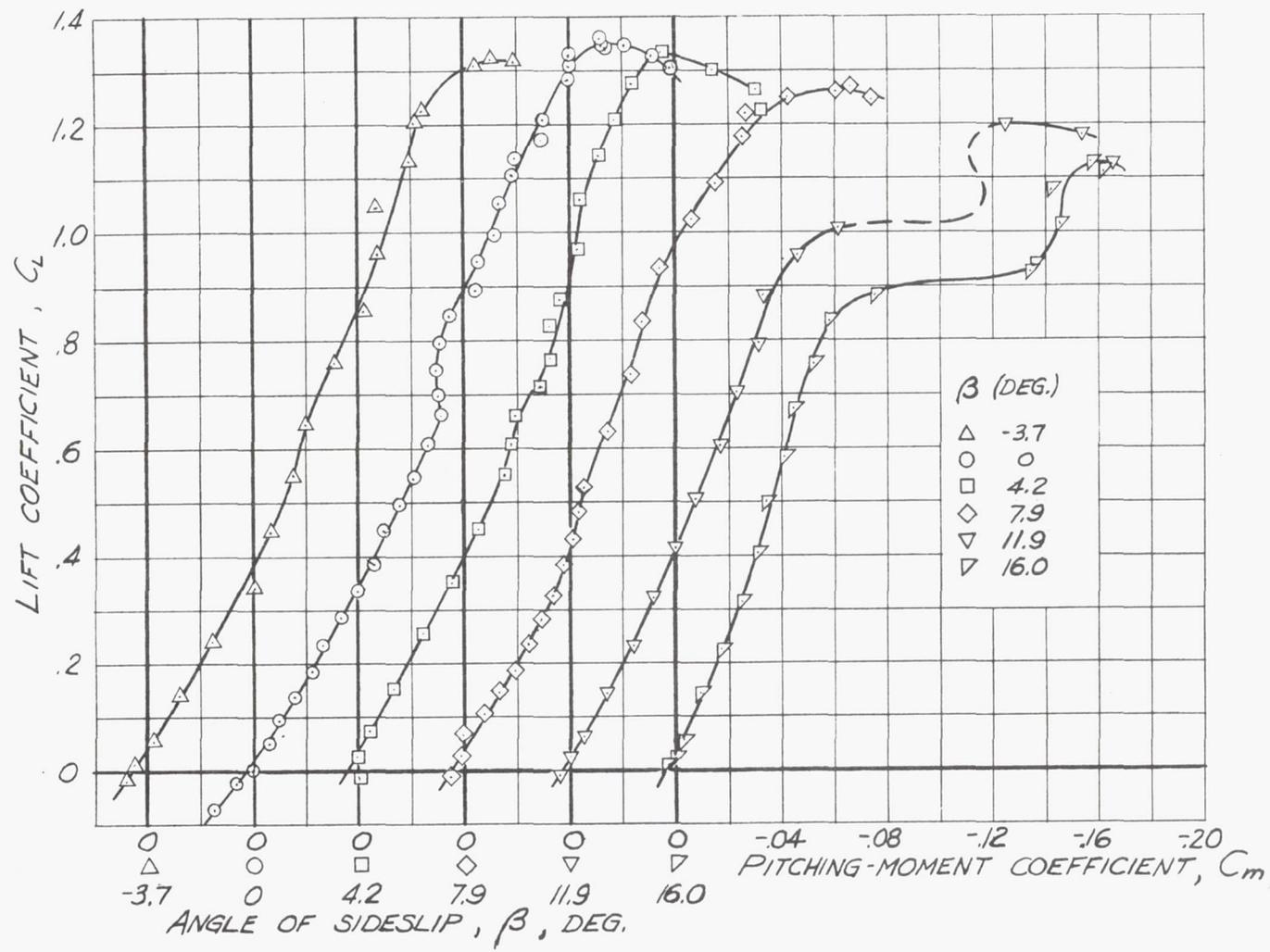
FIGURE 8.- CONTINUED.

(C) C_L vs C_m

FIGURE 8.- CONTINUED.

NATIONAL ADVISORY COMMITTEE
FOR AERONAUTICS

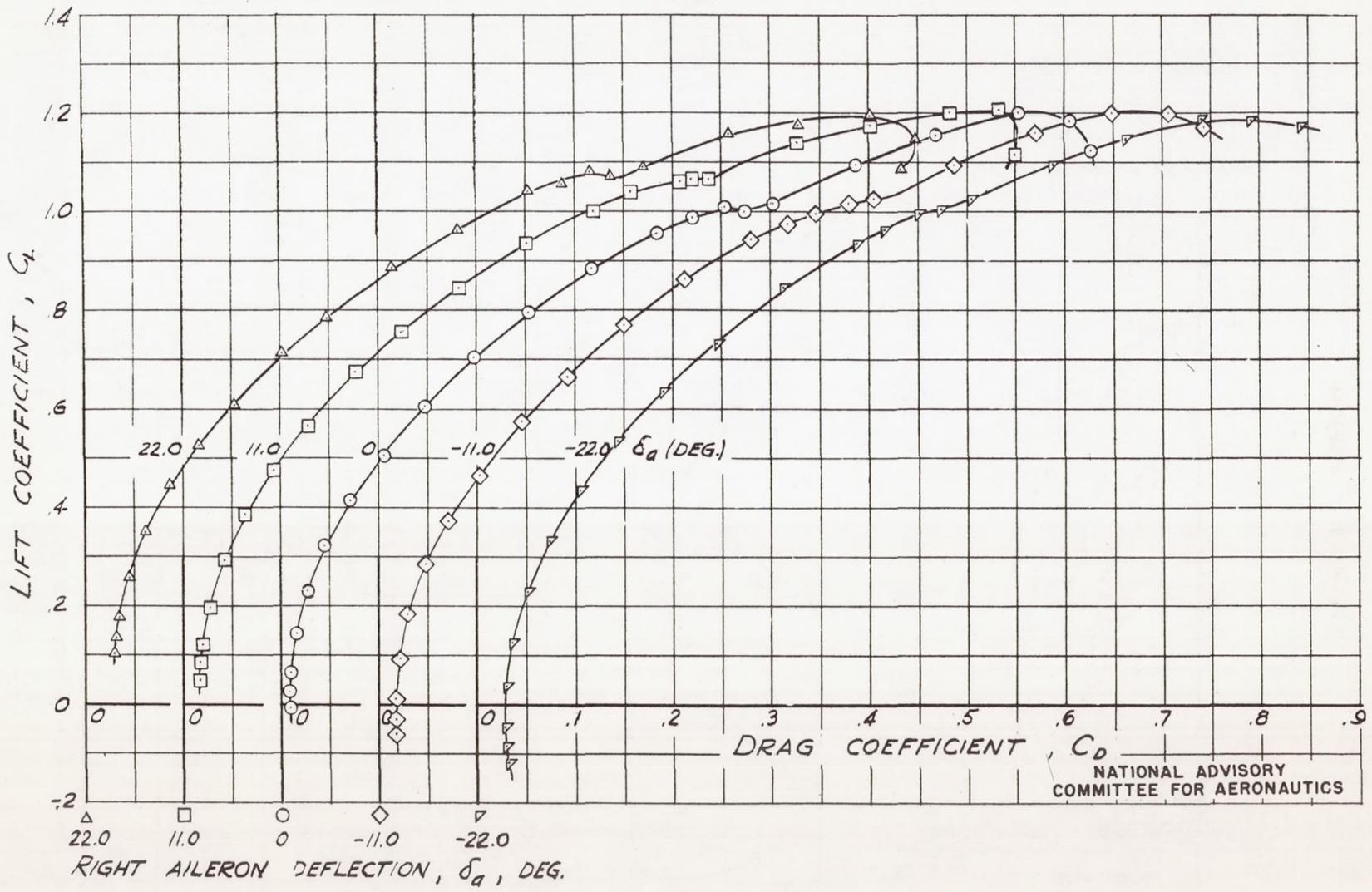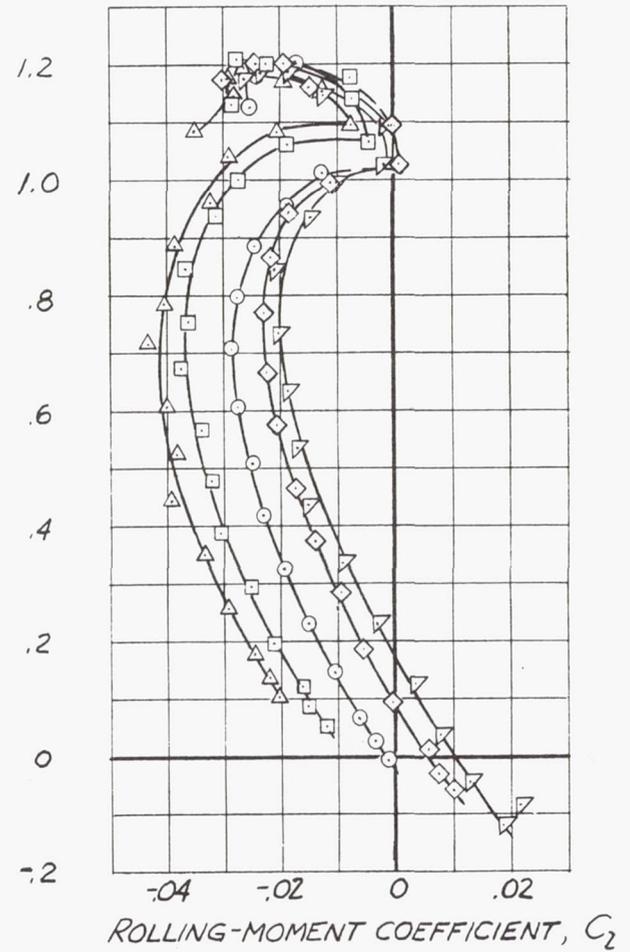β (DEG.)
△ -3.7
○ 0
□ 4.2
◇ 7.9
▽ 11.9
▽ 16.0

ROLLING-MOMENT COEFFICIENT, C_l

YAWING-MOMENT COEFFICIENT, C_n

SIDE-FORCE COEFFICIENT, C_Y
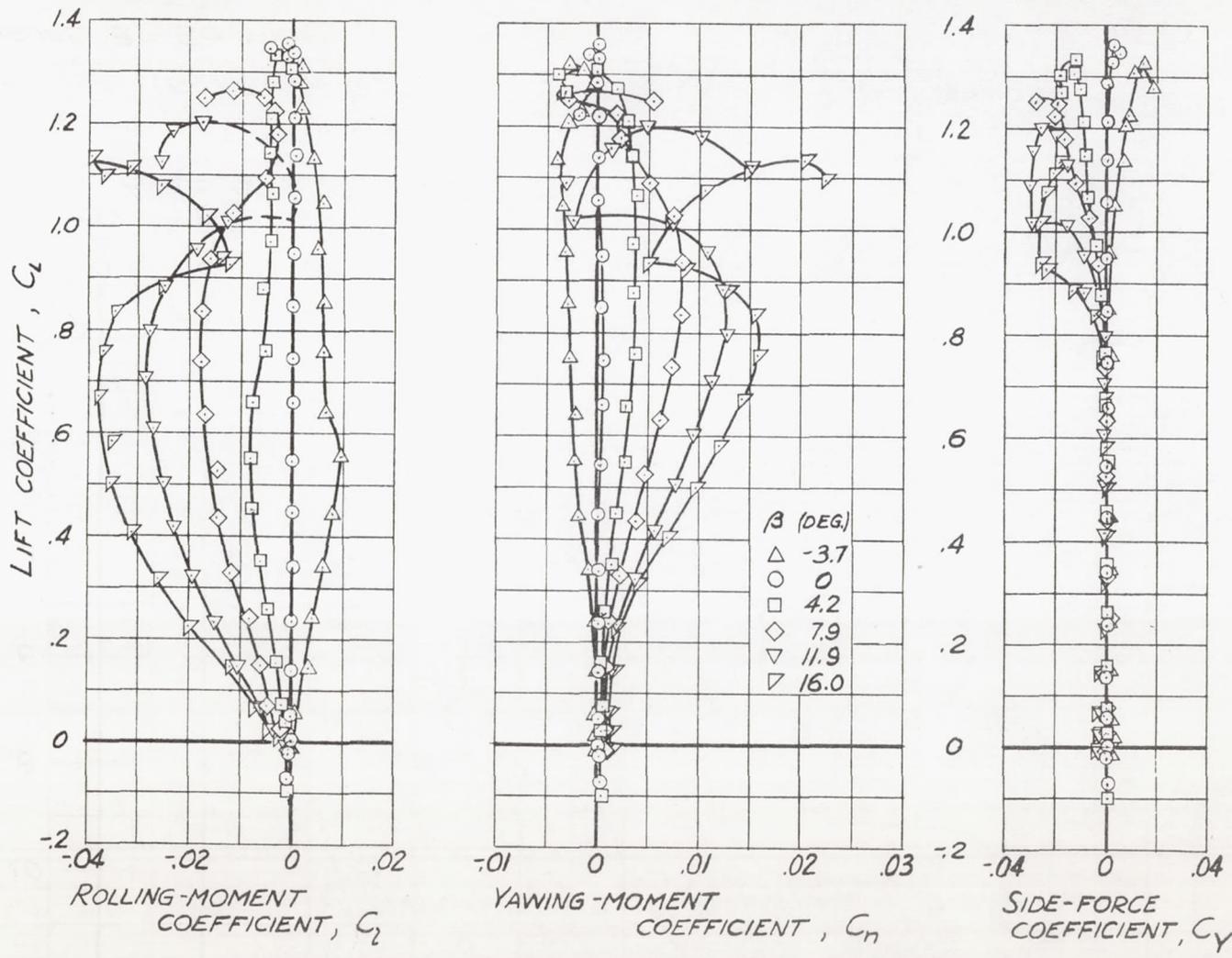
(d) C_L vs C_l, C_n, AND C_Y

FIGURE 8.- CONCLUDED.

NATIONAL ADVISORY COMMITTEE
FOR AERONAUTICS

Fig. 8 d

Fig. 9 a

Reynolds number = 15.4×10^6

β (DEG.)

-3.7   0   7.9   11.9

NATIONAL ADVISORY
COMMITTEE FOR AERONAUTICS

△	○	◻	◇
-3.7	0	7.9	11.9
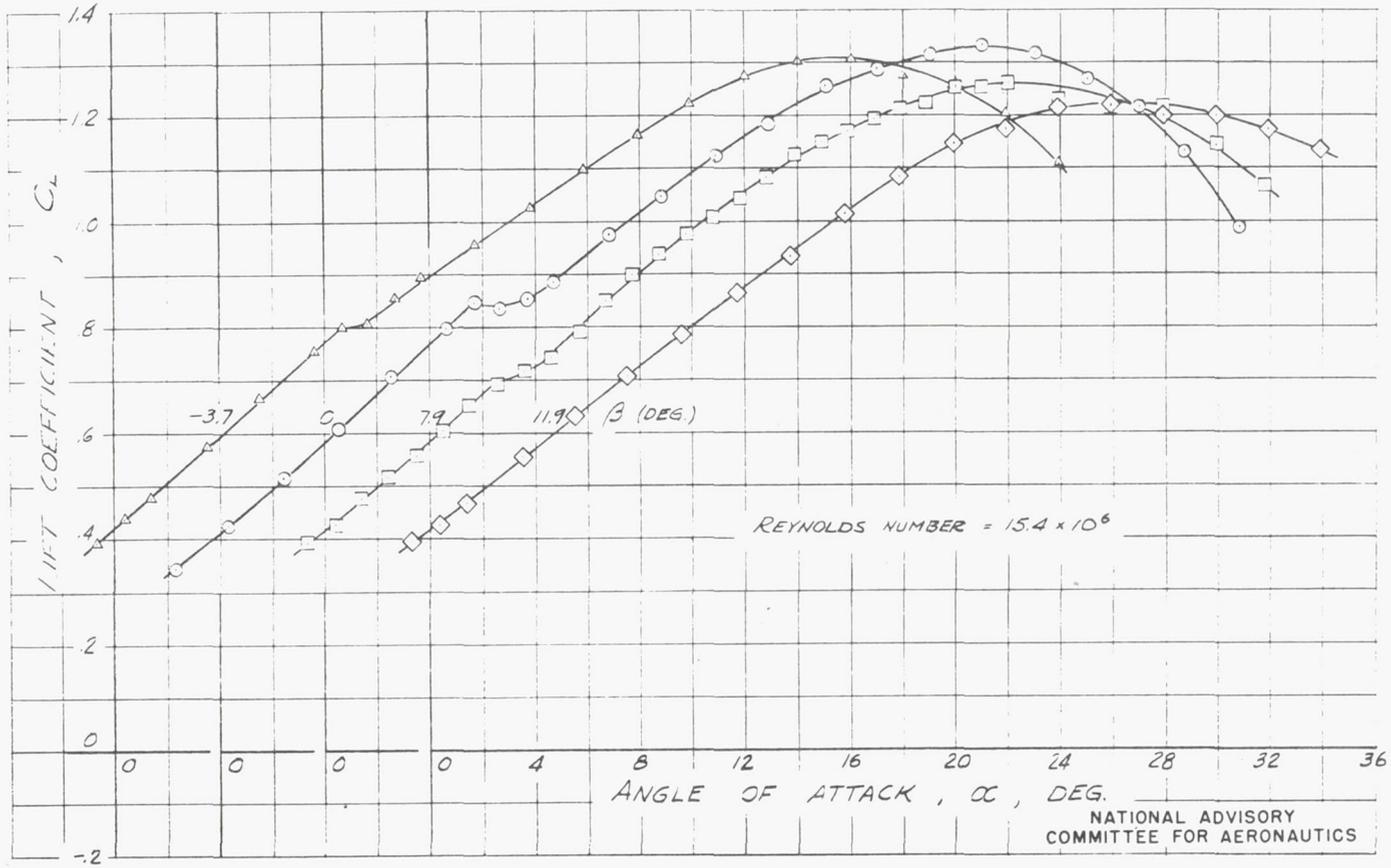
ANGLE OF SIDESLIP, β, DEG

NOTE DISPLACED SCALES

(a) C_L VS α

FIGURE 9 .- AERODYNAMIC CHARACTERISTICS OF THE TRIANGULAR WING WITH 18.5 PERCENT AREA SPLIT FLAPS DEFLECTED 44.5° AT ANGLES OF SIDESLIP FROM -3.7° TO 11.9°.

(b) C_L vs C_D

FIGURE 9.- CONTINUED.

Fig. 9 b

Fig. 9 c

β (DEG.)
△ -3.7
○   0
□   7.9
◇ 11.9

PITCHING-MOMENT
COEFFICIENT, C_m

ROLLING-MOMENT
COEFFICIENT, C_l

YAWING-MOMENT
COEFFICIENT, C_n

SIDE-FORCE
COEFFICIENT, C_Y

LIFT COEFFICIENT, C_L

△   ○   □   ◇
-3.7   0   7.9   11.9
ANGLE OF SIDESLIP, β, DEG.

NATIONAL ADVISORY COMMITTEE
FOR AERONAUTICS
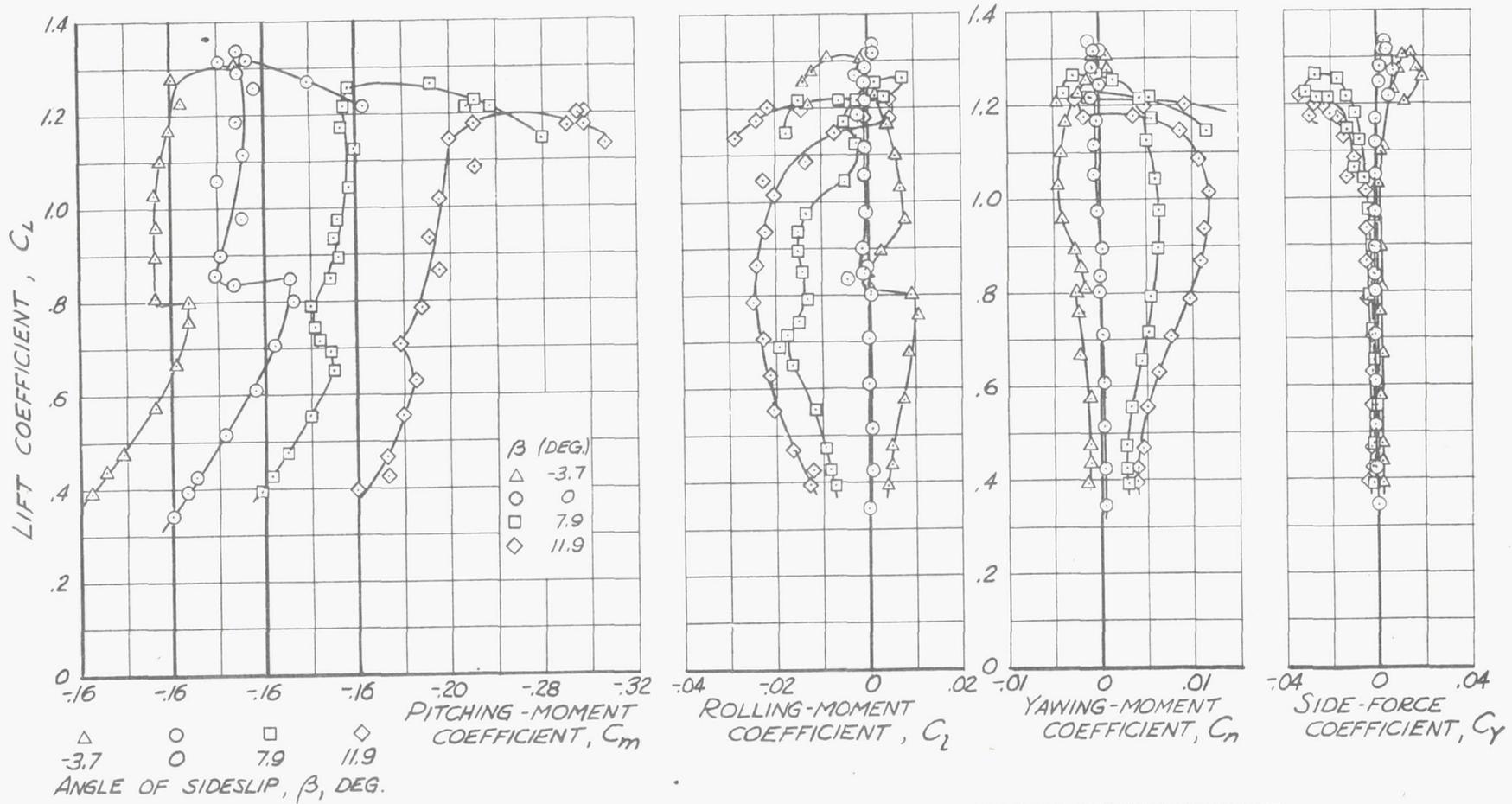
(c) C_L vs C_m, C_l, C_n, AND C_Y

FIGURE 9.- CONCLUDED.

NATIONAL ADVISORY
COMMITTEE FOR AERONAUTICS

RIGHT AILERON DEFLECTION, δ_a, DEG.
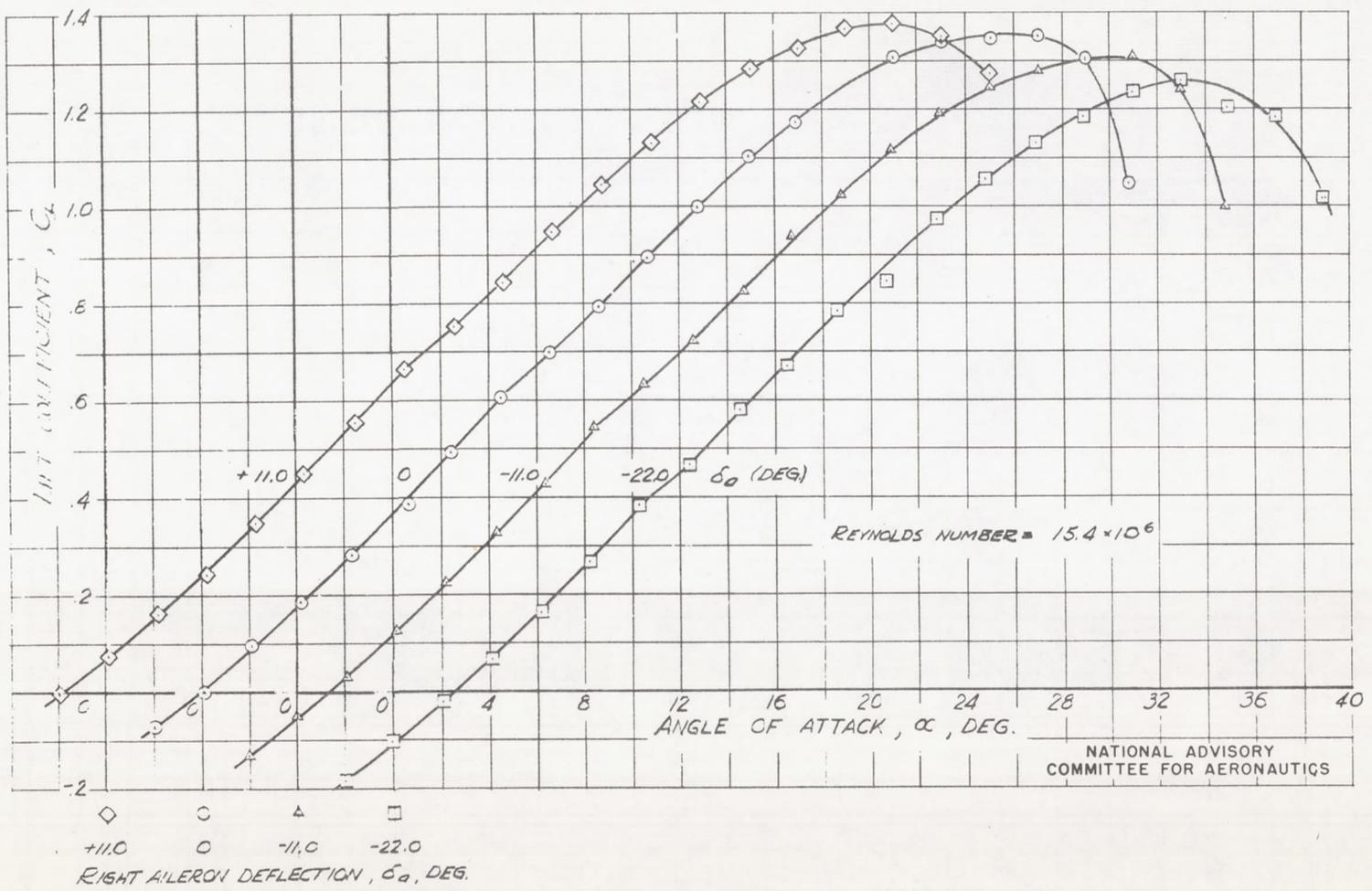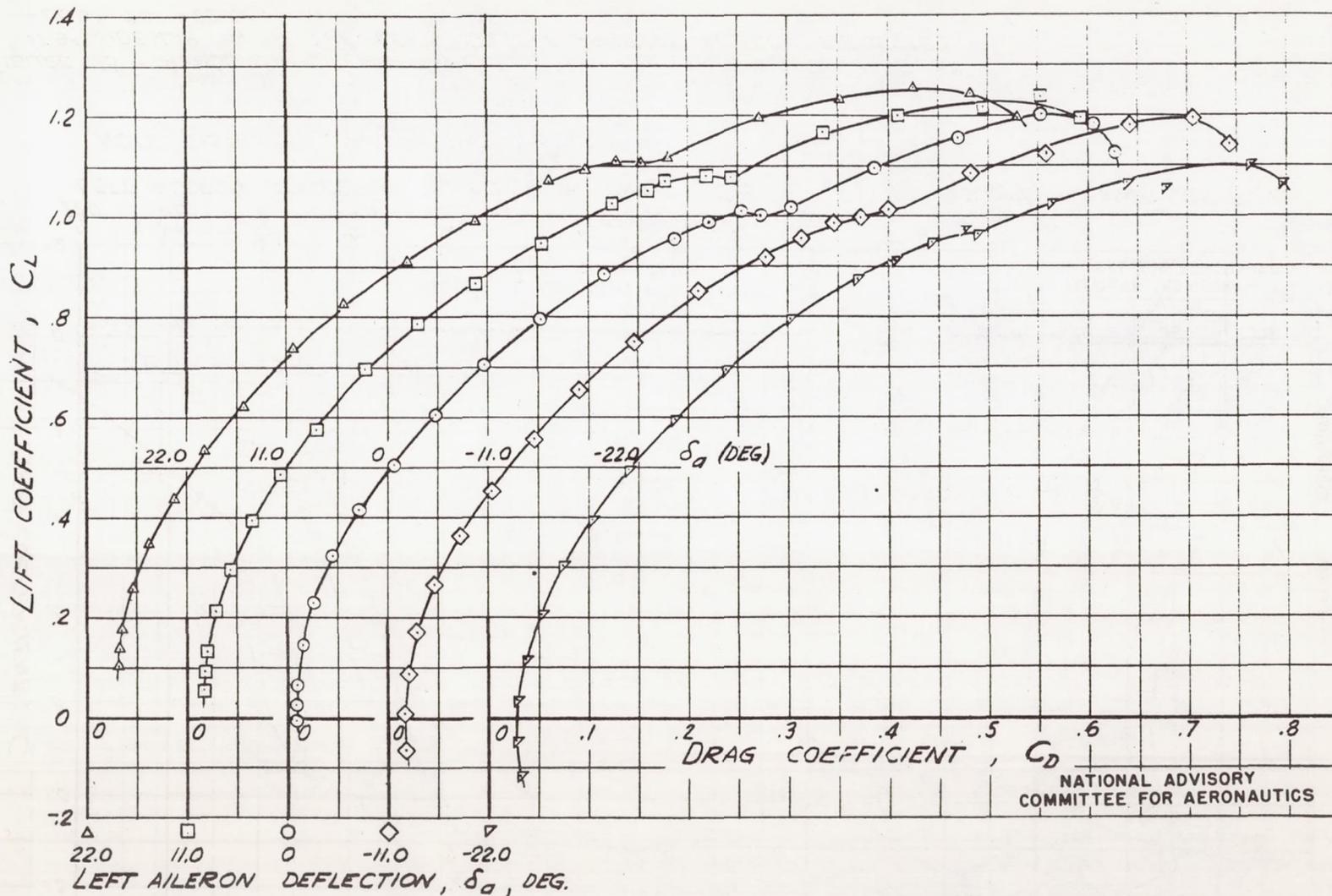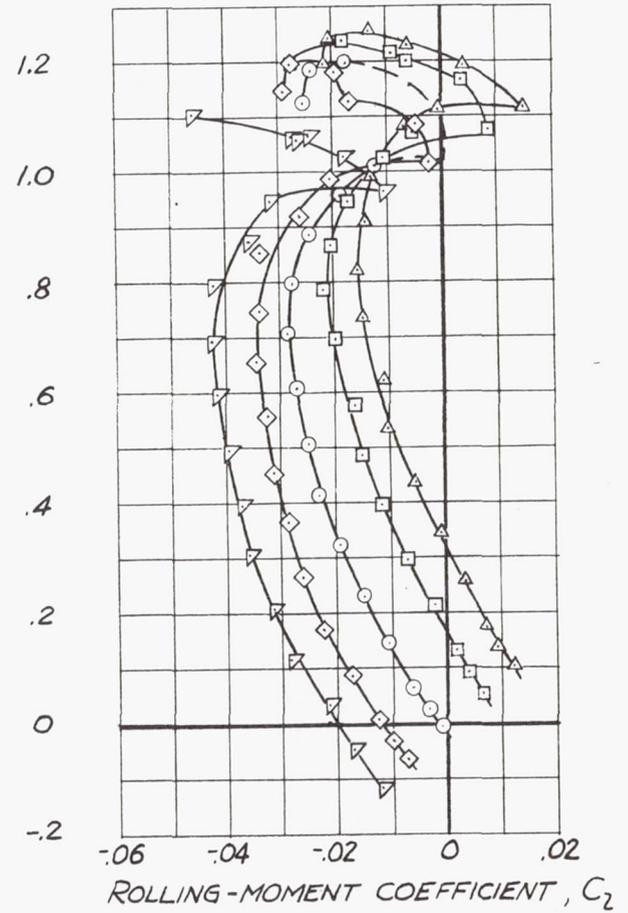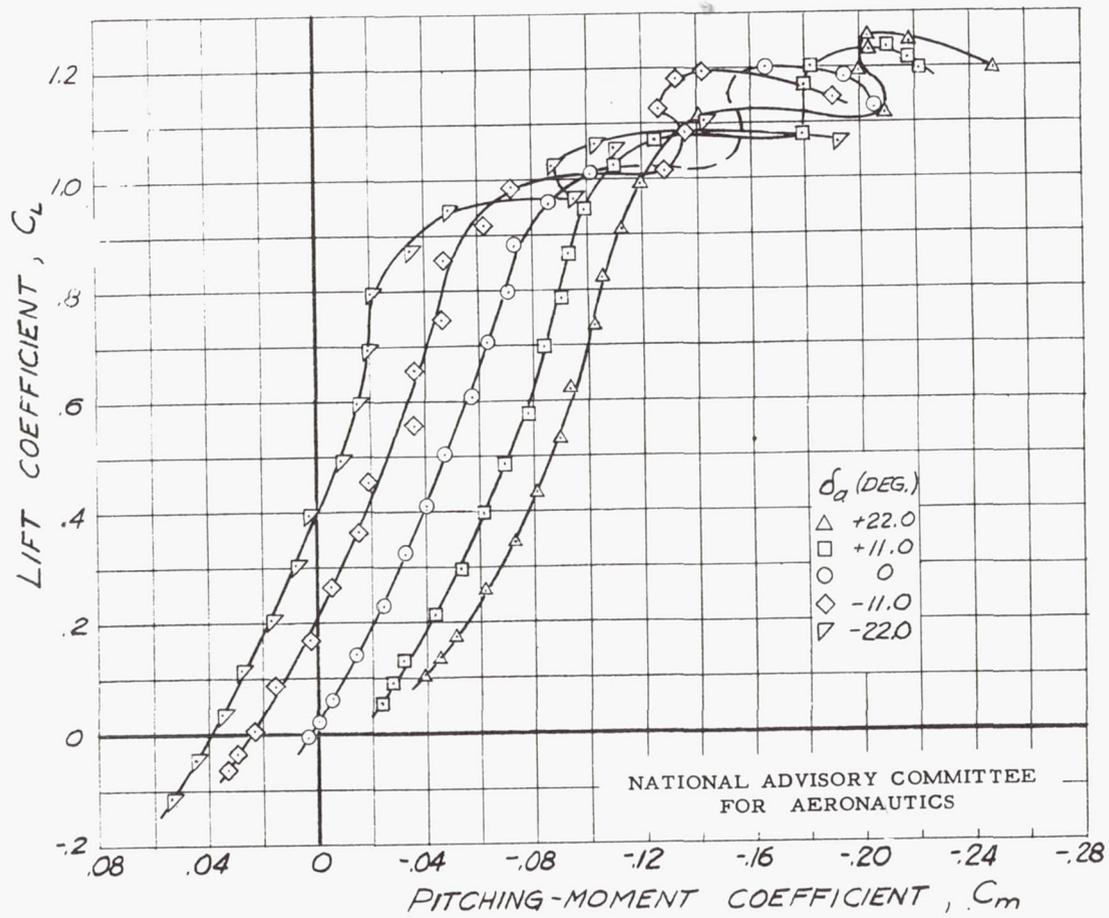
NOTE DISPLACED SCALES

(a) C_L vs α

FIGURE 10.- AERODYNAMIC CHARACTERISTICS OF THE TRIANGULAR WING
AT 0° SIDESLIP WITH RIGHT SPLIT-FLAP-TYPE AILERON DEFLECTED
-22.0° TO 11.0°.

Fig. 10 a
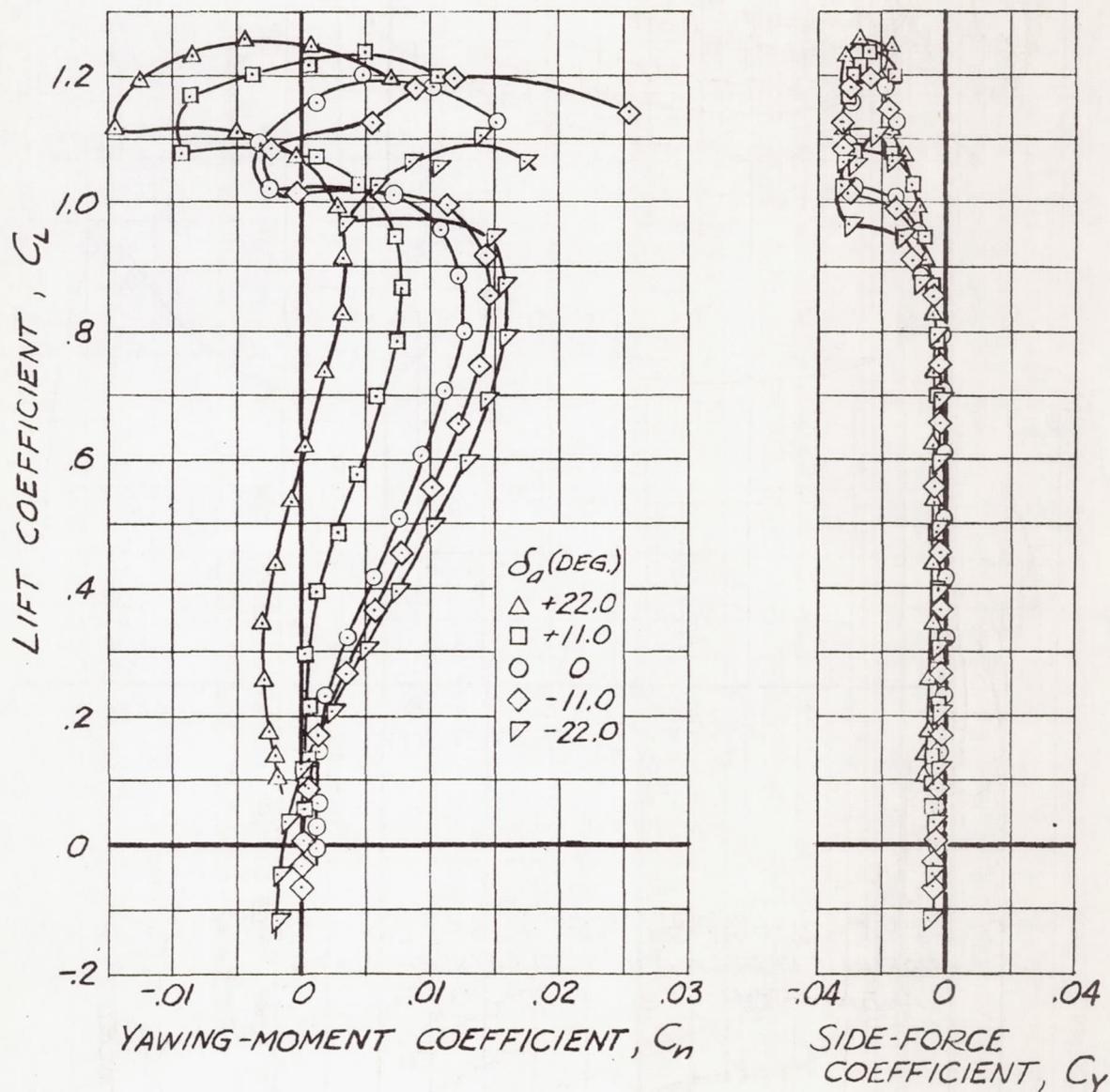
Fig. 10 b

REYNOLDS NUMBER 15.4 × 10⁵

δₐ (DEG.)

LIFT COEFFICIENT, C_L

DRAG COEFFICIENT, C_D

+11.0   0   -11.0   -22.0

RIGHT AILERON DEFLECTION, δ_a, DEG.

(b) C_L vs C_D

NATIONAL ADVISORY
COMMITTEE FOR AERONAUTICS
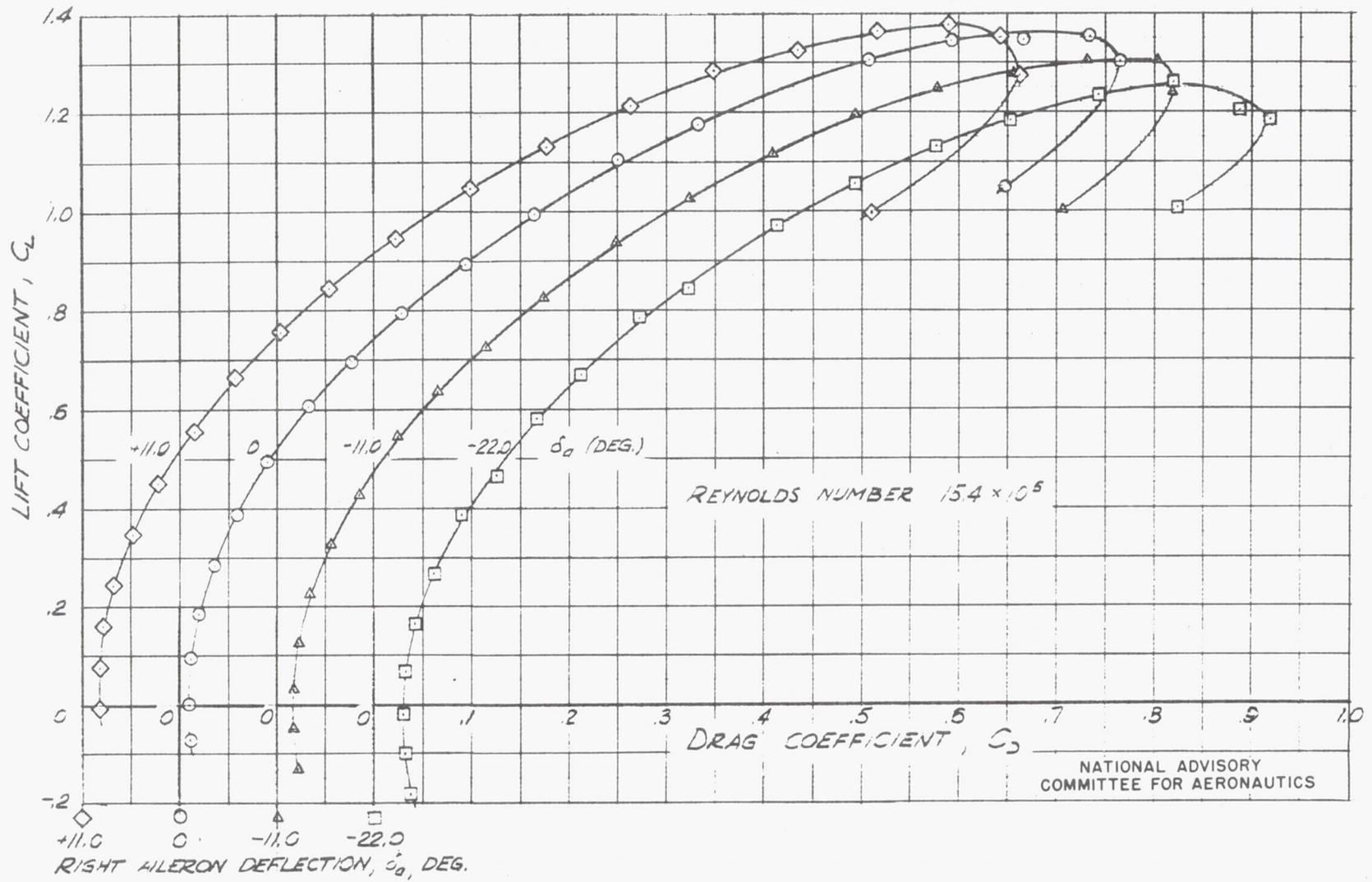
FIGURE 10.- CONTINUED.
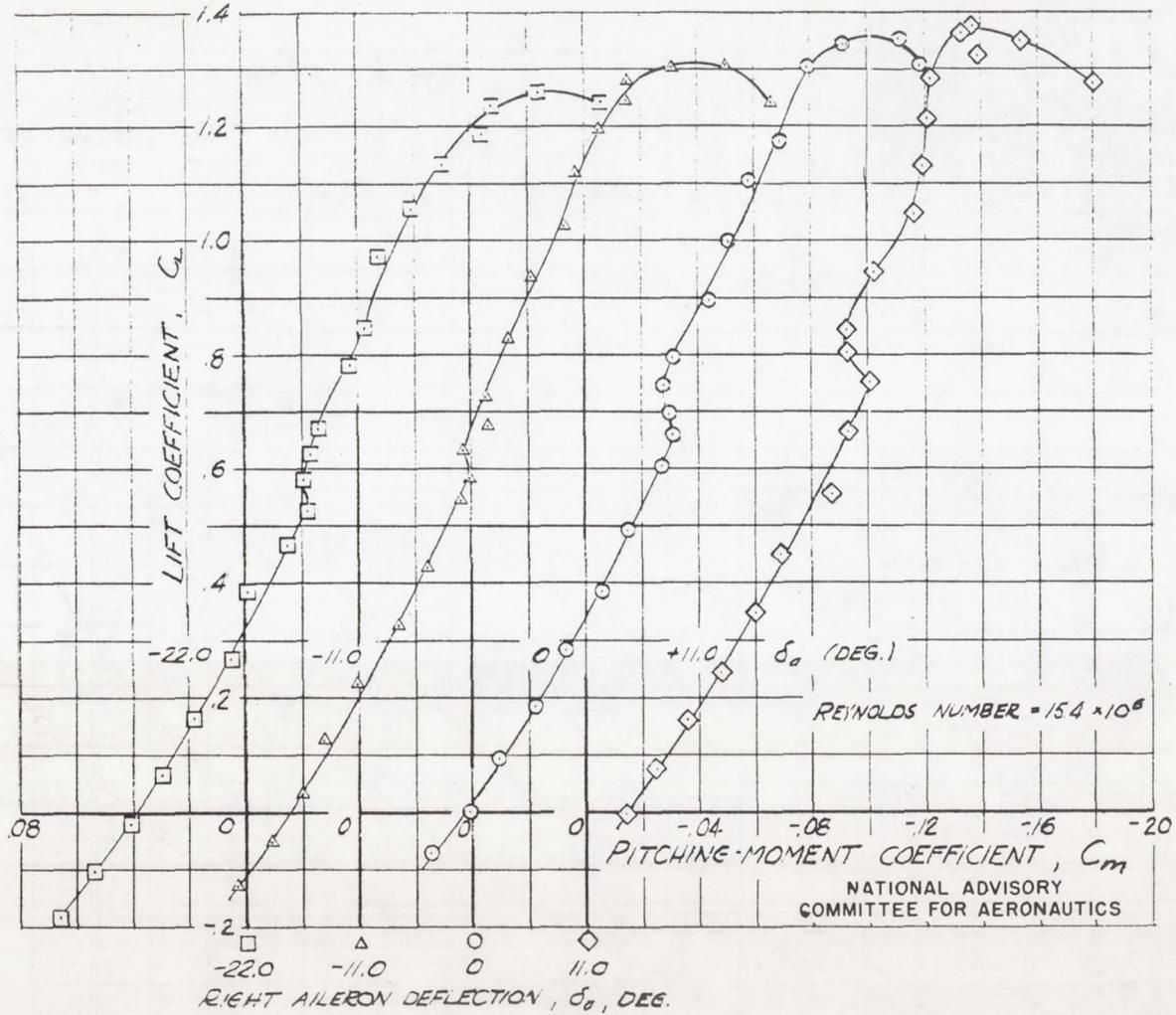
(c) C_L vs C_m

FIGURE 10. - CONTINUED

Fig. 10 c

Fig. 10 d   NACA RM No. A-7F06

(d) C_L vs C_l, C_n and C_y

FIGURE 10.- CONCLUDED.
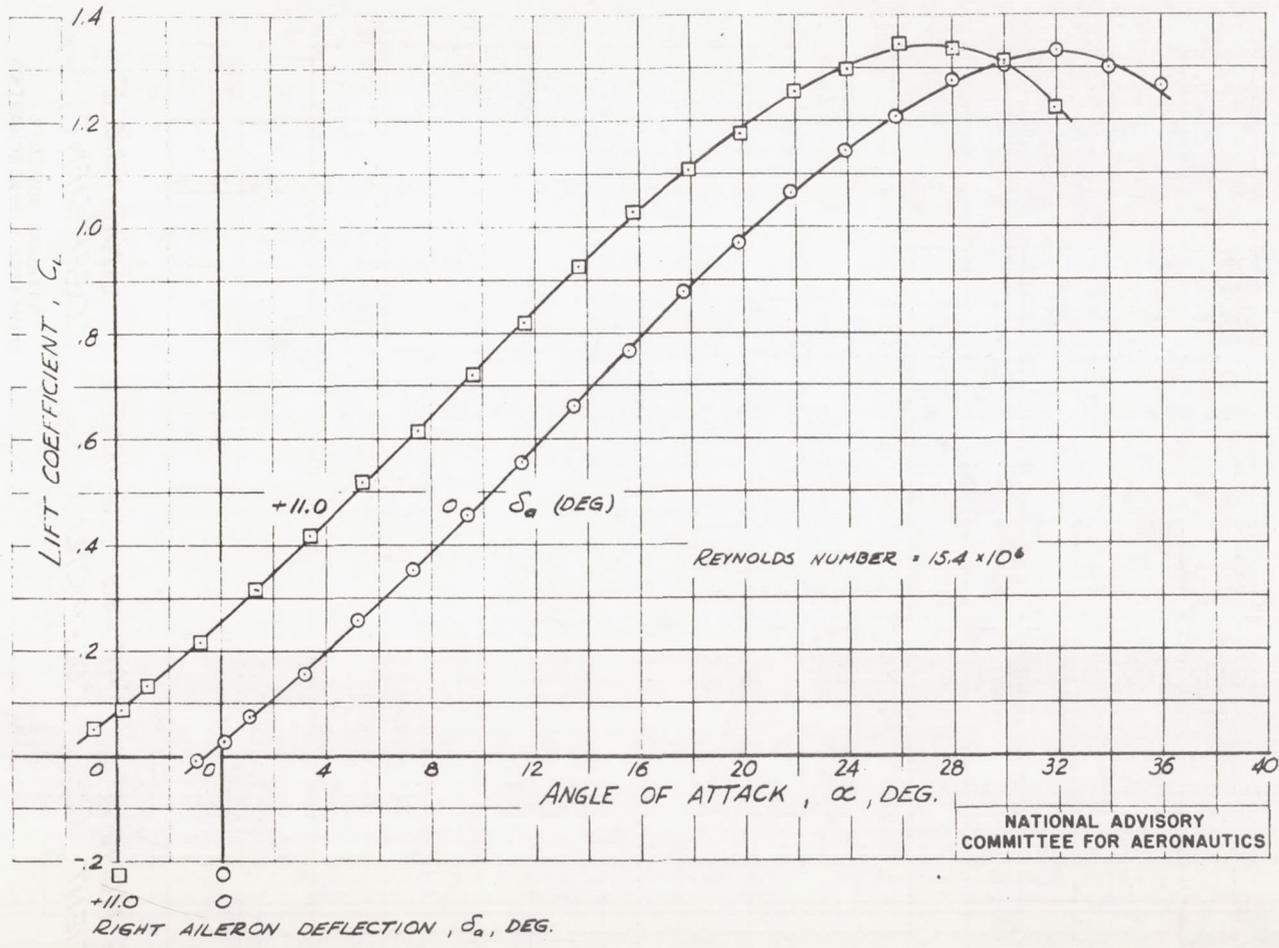
(a) C_L vs α

FIGURE 11.- AERODYNAMIC CHARACTERISTICS OF THE TRIANGULAR WING AT 4.2° SIDESLIP WITH RIGHT SPLIT-FLAP-TYPE AILERON DEFLECTED 0° AND 11.0°.
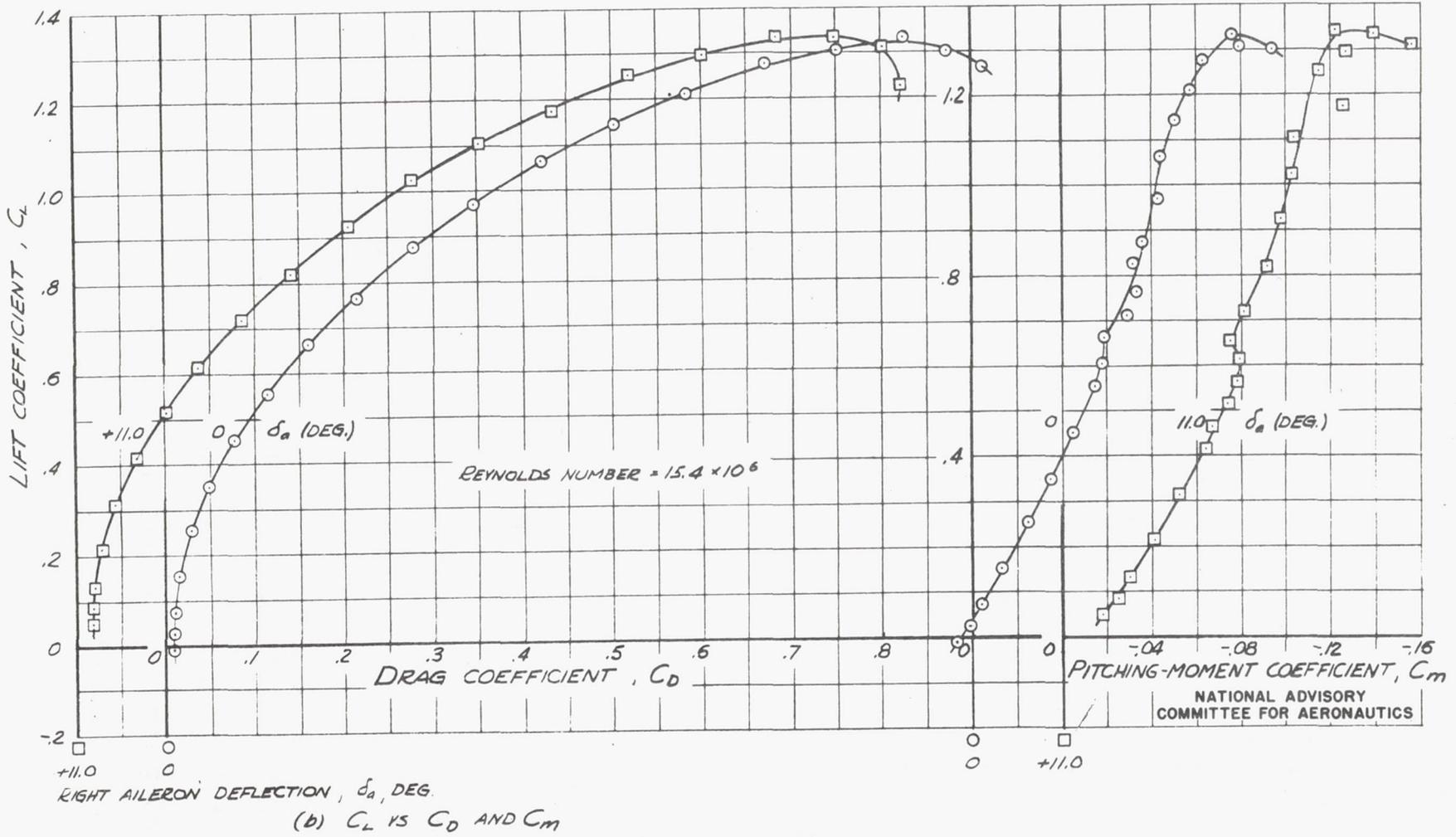
Fig. 11 b

(b) C_L vs C_D and C_m

FIGURE 11.- CONTINUED.

ROLLING-MOMENT COEFFICIENT, C_l

YAWING-MOMENT COEFFICIENT, C_n

SIDE-FORCE COEFFICIENT, C_Y
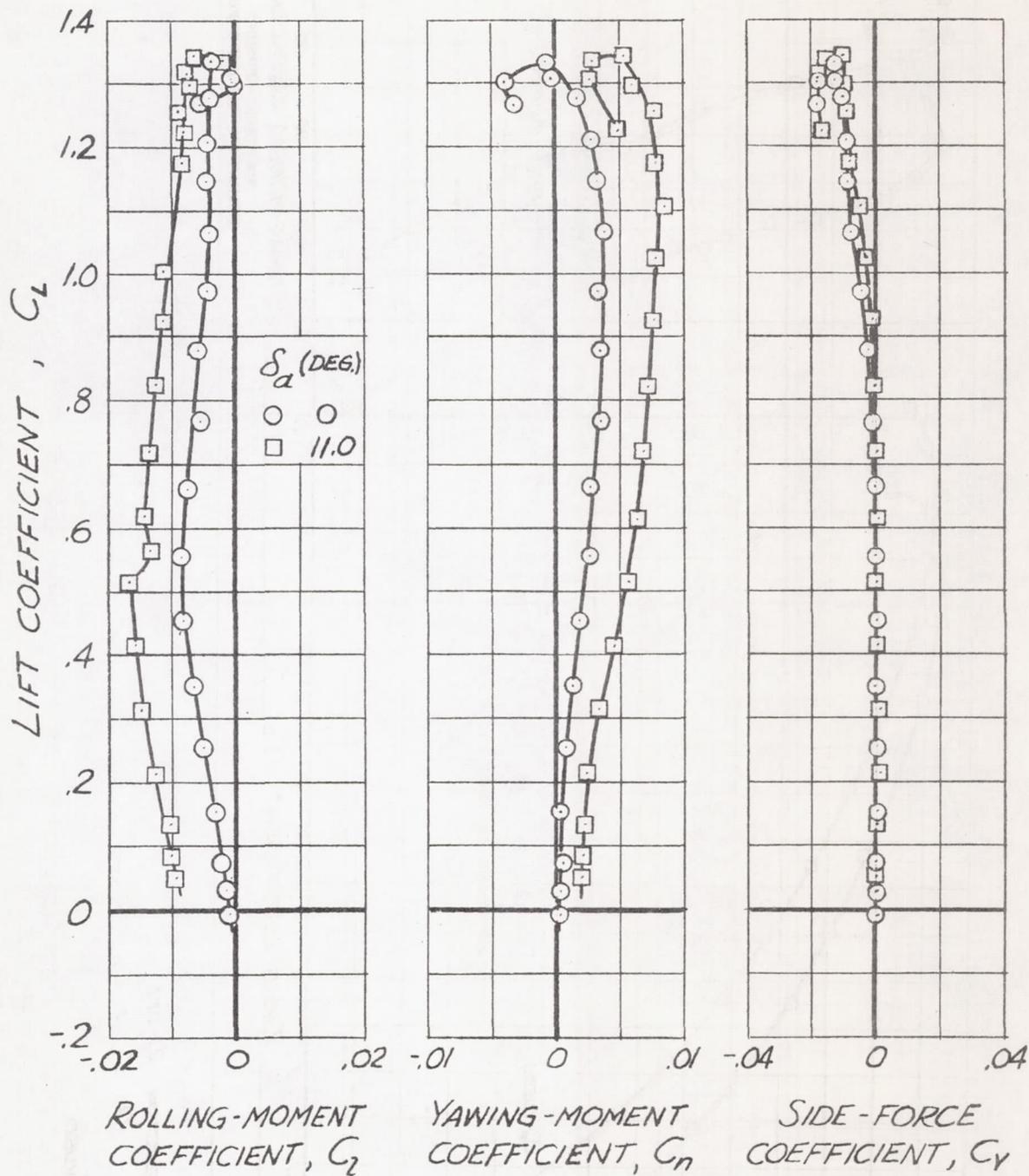
NATIONAL ADVISORY COMMITTEE
FOR AERONAUTICS

(c) C_L vs C_l, C_n and C_Y.

FIGURE 11. — CONCLUDED.

Fig. 12 a

δ_a (DEG.)

REYNOLDS NUMBER = 15.4 × 10⁶

RIGHT AILERON DEFLECTION, δ_a, DEG.

NOTE DISPLACED SCALES
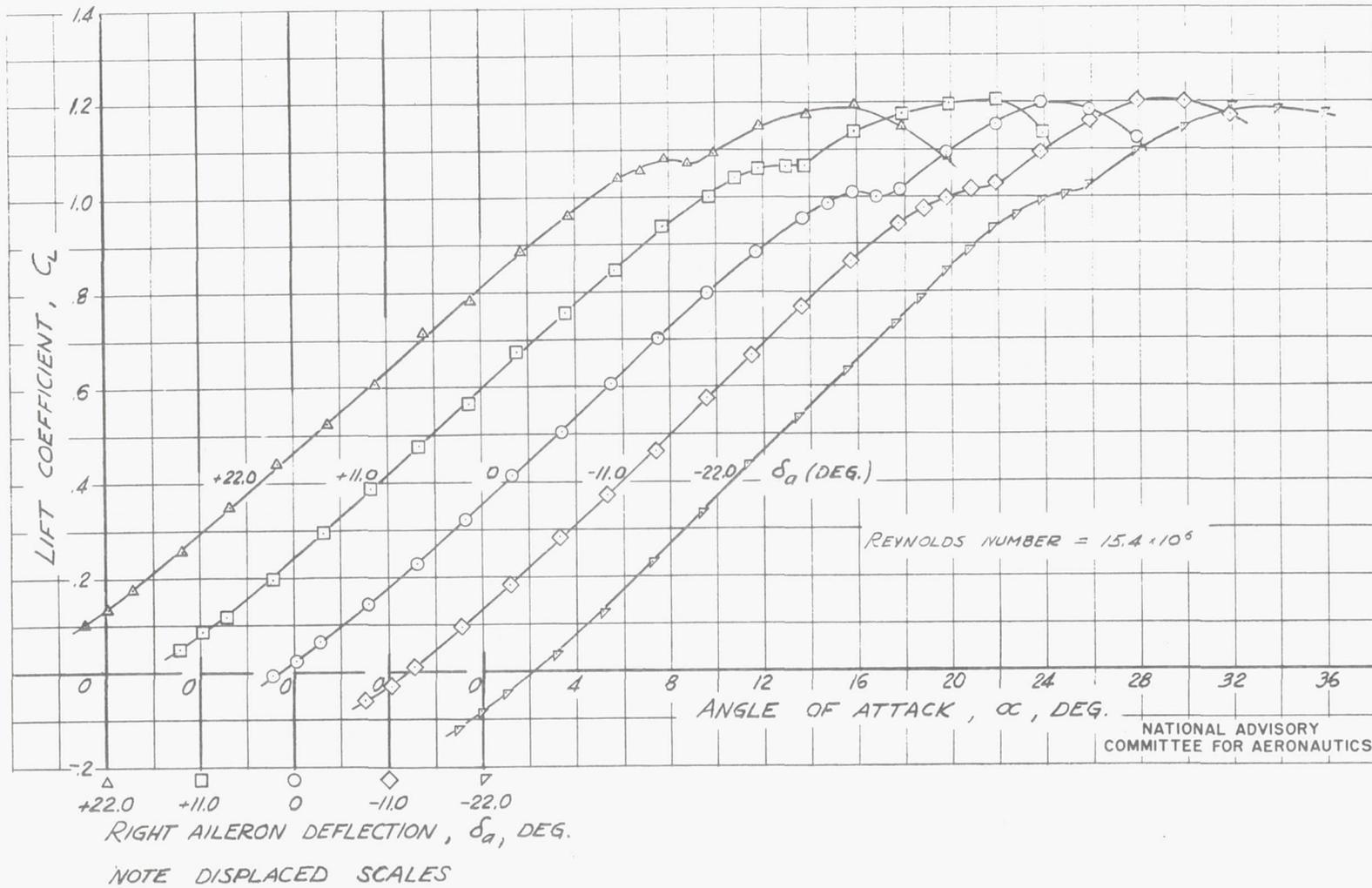
(a) C_L VS α

FIGURE 12.- AERODYNAMIC CHARACTERISTICS OF THE TRIANGULAR WING
AT 11.9° SIDESLIP WITH THE RIGHT SPLIT-FLAP-TYPE AILERON
DEFLECTED -22.0° TO +22.0°.

NATIONAL ADVISORY
COMMITTEE FOR AERONAUTICS

Fig. 12 b

FIGURE 12.- CONTINUED.

δ_a (DEG.)

△ +22.0
□ +11.0
○ 0
◇ −11.0
▽ −22.0

LIFT COEFFICIENT, C_L

PITCHING-MOMENT COEFFICIENT, C_m

ROLLING-MOMENT COEFFICIENT, C_l

(C) C_L VS C_m AND C_l

FIGURE 12. - CONTINUED.
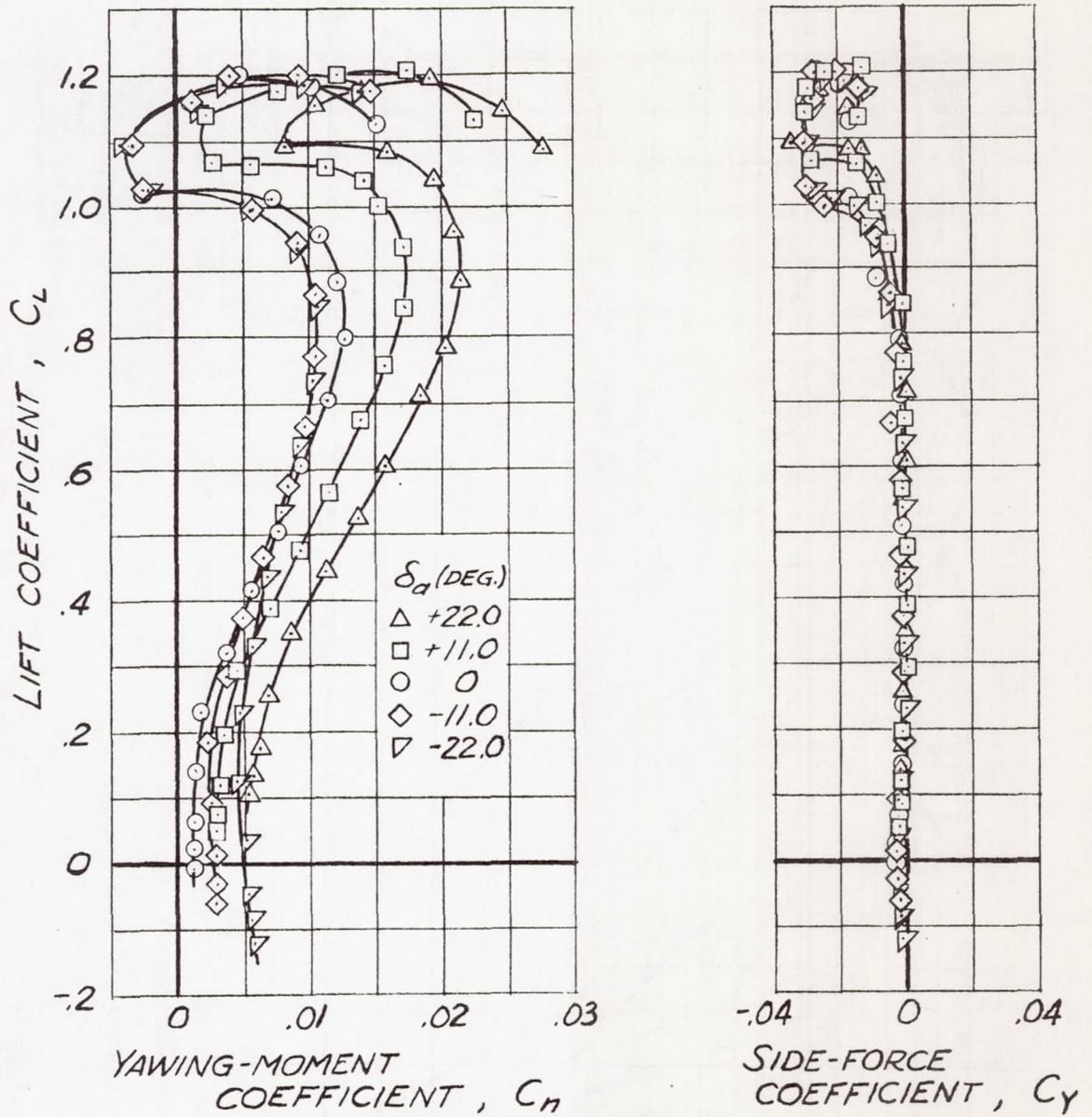
NATIONAL ADVISORY COMMITTEE
FOR AERONAUTICS

(d) C_L vs C_n AND C_Y

FIGURE 12. - CONCLUDED.

Fig. 13 a

NATIONAL ADVISORY
COMMITTEE FOR AERONAUTICS

LEFT AILERON DEFLECTION, δ_a, DEG.

NOTE DISPLACED SCALES

(a) C_L vs α
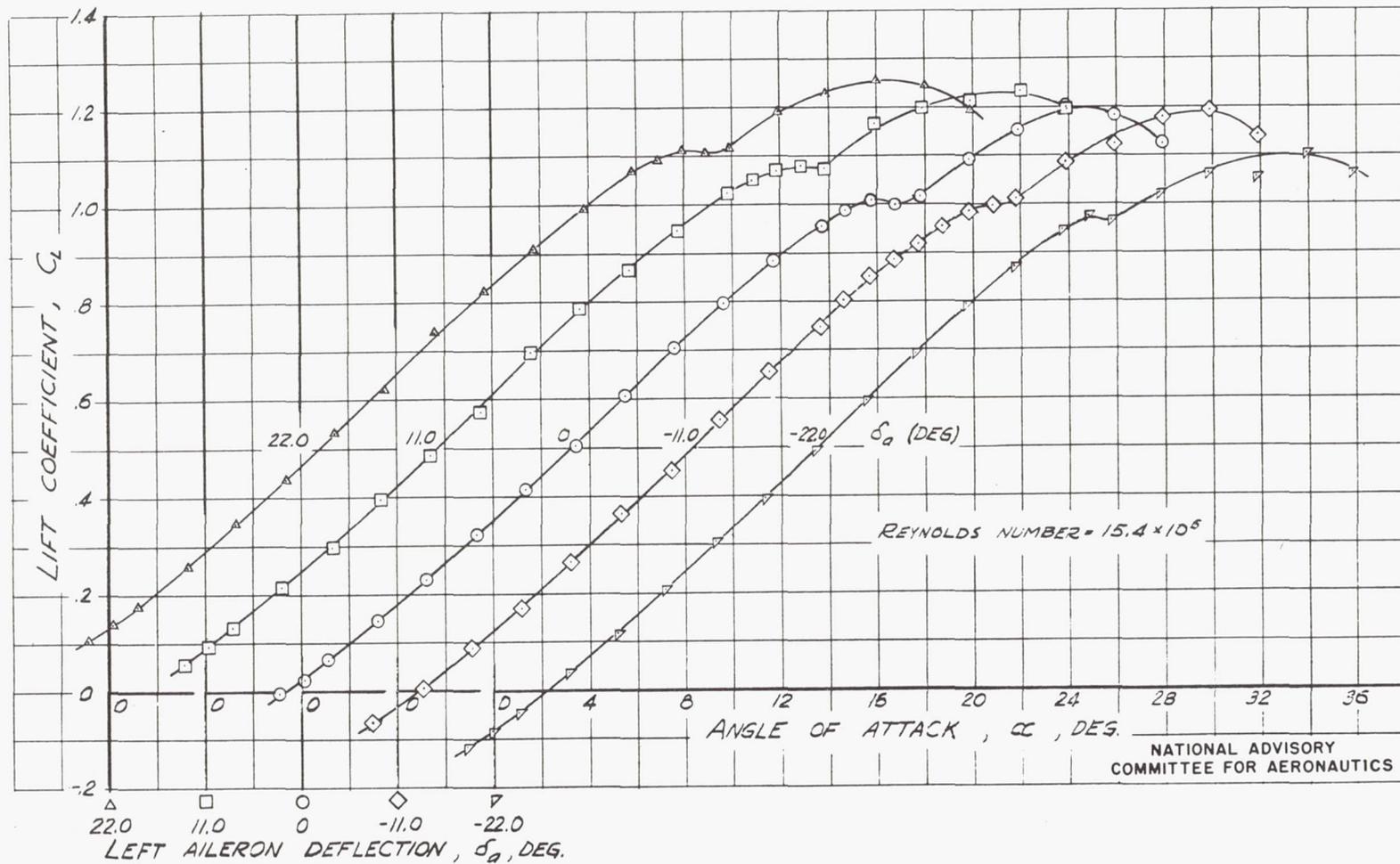
FIGURE 13.- AERODYNAMIC CHARACTERISTICS OF THE TRIANGULAR WING AT
11.9° SIDESLIP WITH THE LEFT SPLIT-FLAP-TYPE AILERON DEFLECTED
-22.0° TO +22.0°.

(b) C_L vs C_D

FIGURE 13.- CONTINUED.

Fig. 13 b

Fig. 13 c

δ_a (DEG.)
△ +22.0
□ +11.0
○   0
◇ −11.0
▽ −22.0

NATIONAL ADVISORY COMMITTEE
FOR AERONAUTICS

LIFT COEFFICIENT , C_L

PITCHING-MOMENT COEFFICIENT , C_m

ROLLING-MOMENT COEFFICIENT , C_l

(C) C_L vs C_m AND C_l

FIGURE 13.— CONTINUED.

(d) C_L vs C_n and C_Y

FIGURE 13.- CONCLUDED.

Fig. 14

NACA RM No. A-7F06
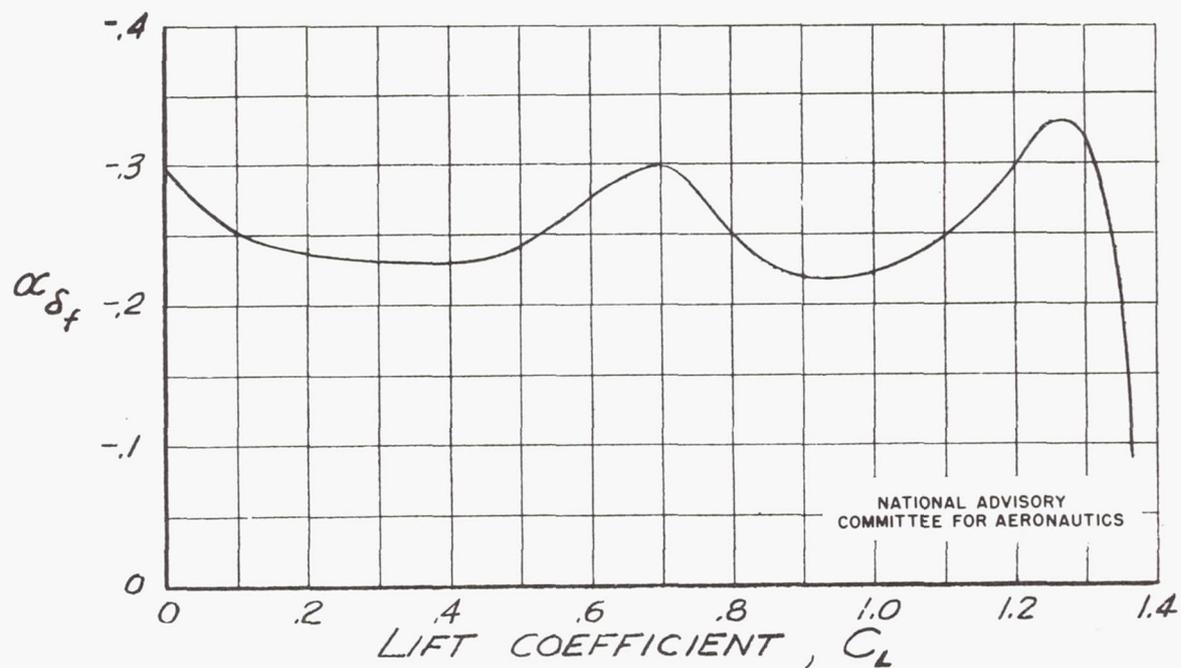
FIGURE 14. - VARIATION OF FLAP EFFECTIVENESS
     PARAMETER WITH LIFT COEFFICIENT. SLOPE
     TAKEN FOR ±2° FLAP DEFLECTION.
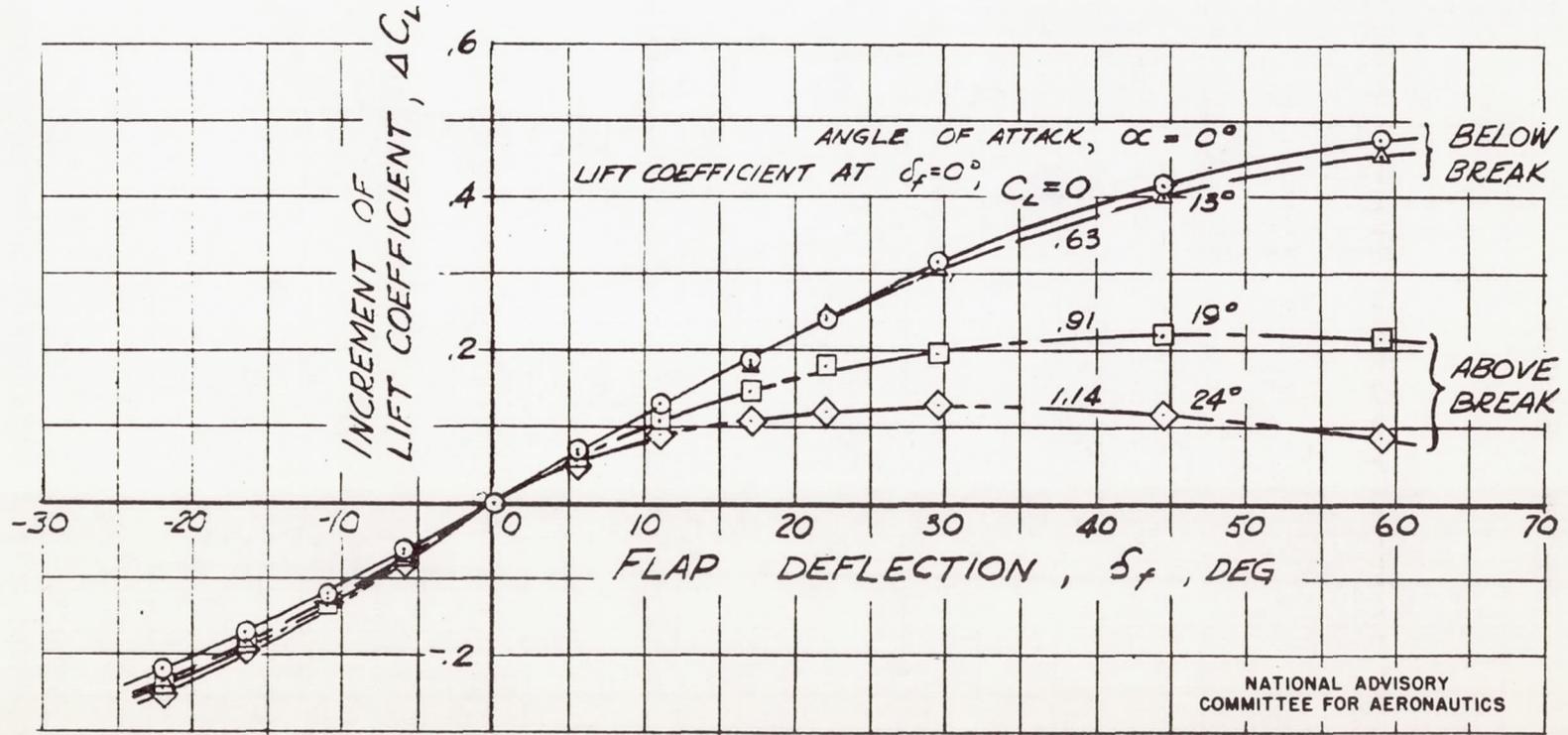
FIGURE 15.—INCREMENT OF LIFT COEFFICIENT DUE TO FLAP
DEFLECTION AT ANGLES OF ATTACK BELOW AND ABOVE
THAT AT WHICH A BREAK APPEARS IN THE LIFT CURVE.

Fig. 15

Fig. 16
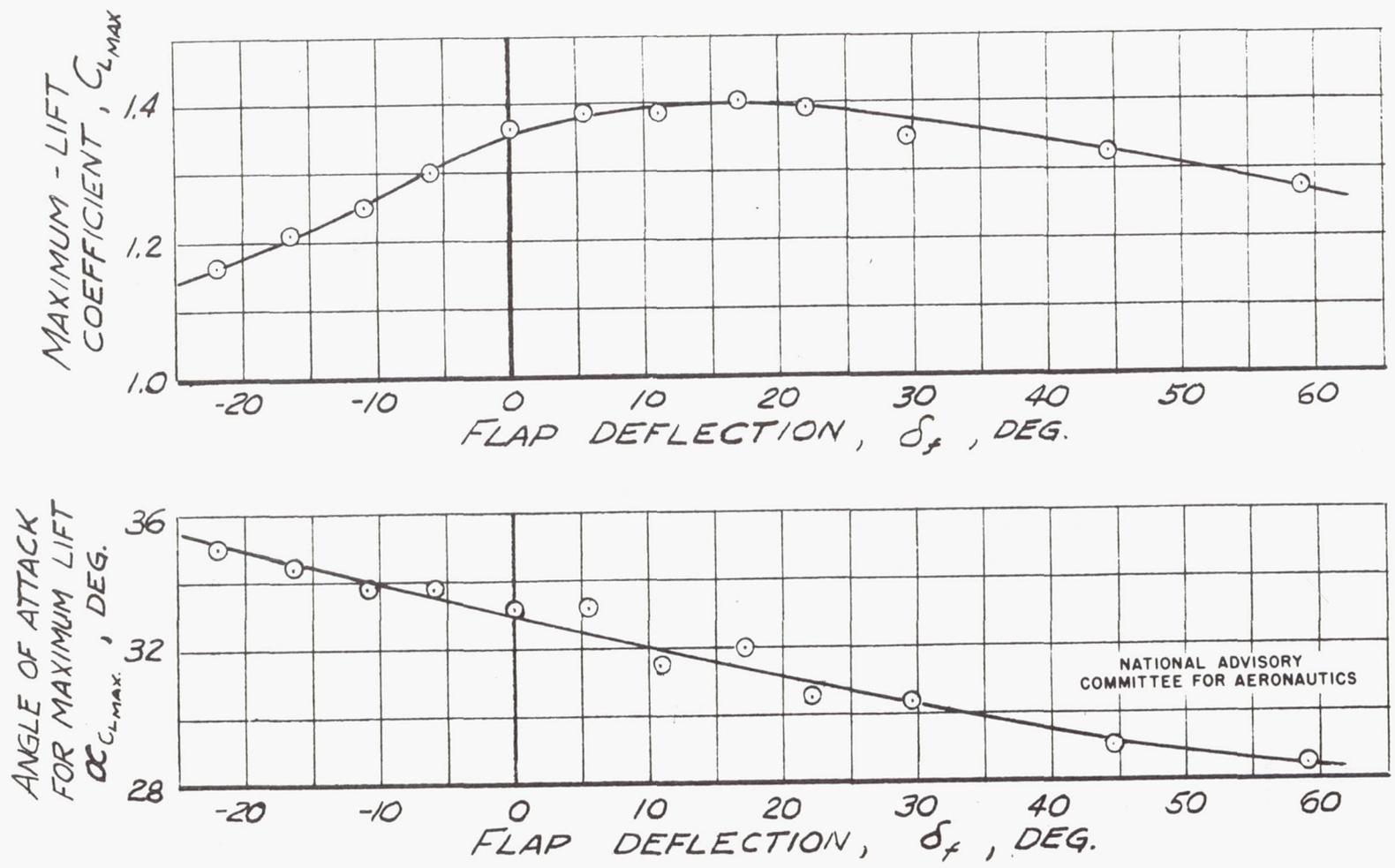
FIGURE 16.- EFFECT OF FLAP DEFLECTION ON MAXIMUM LIFT AND THE
ANGLE OF ATTACK FOR MAXIMUM LIFT.
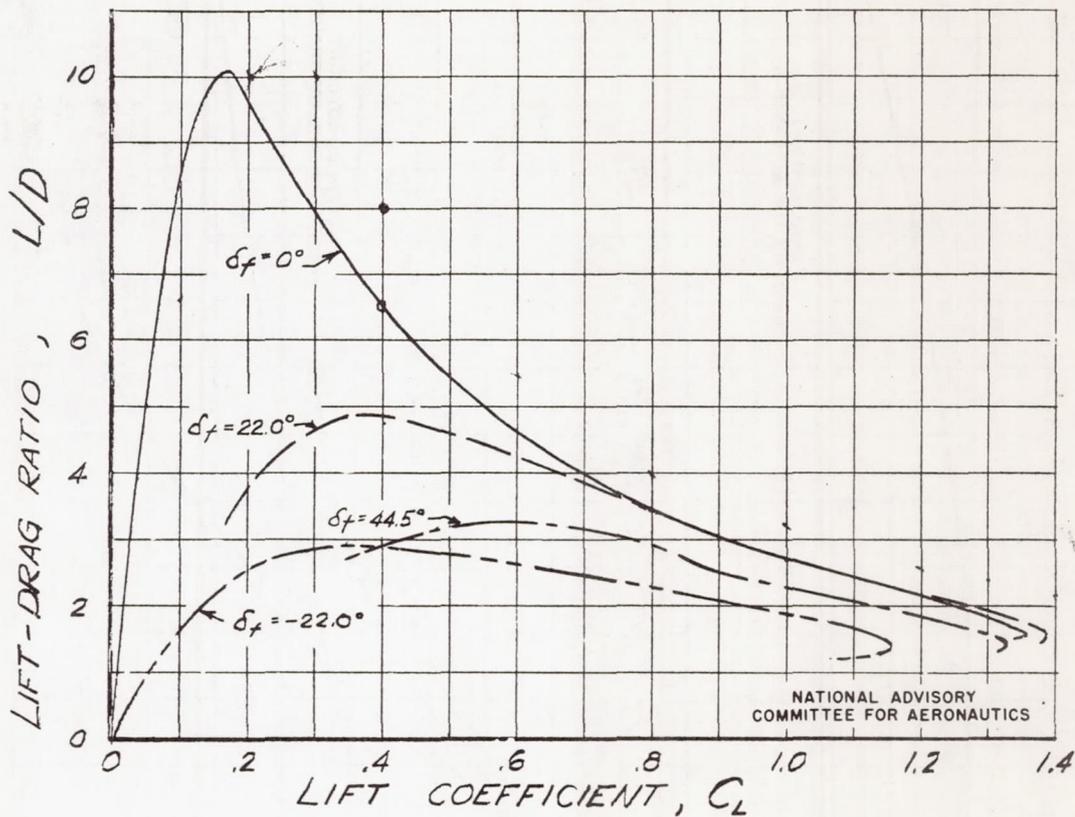
FIGURE 17.- VARIATION OF THE LIFT-DRAG RATIO WITH LIFT COEFFICIENT.

Fig. 18
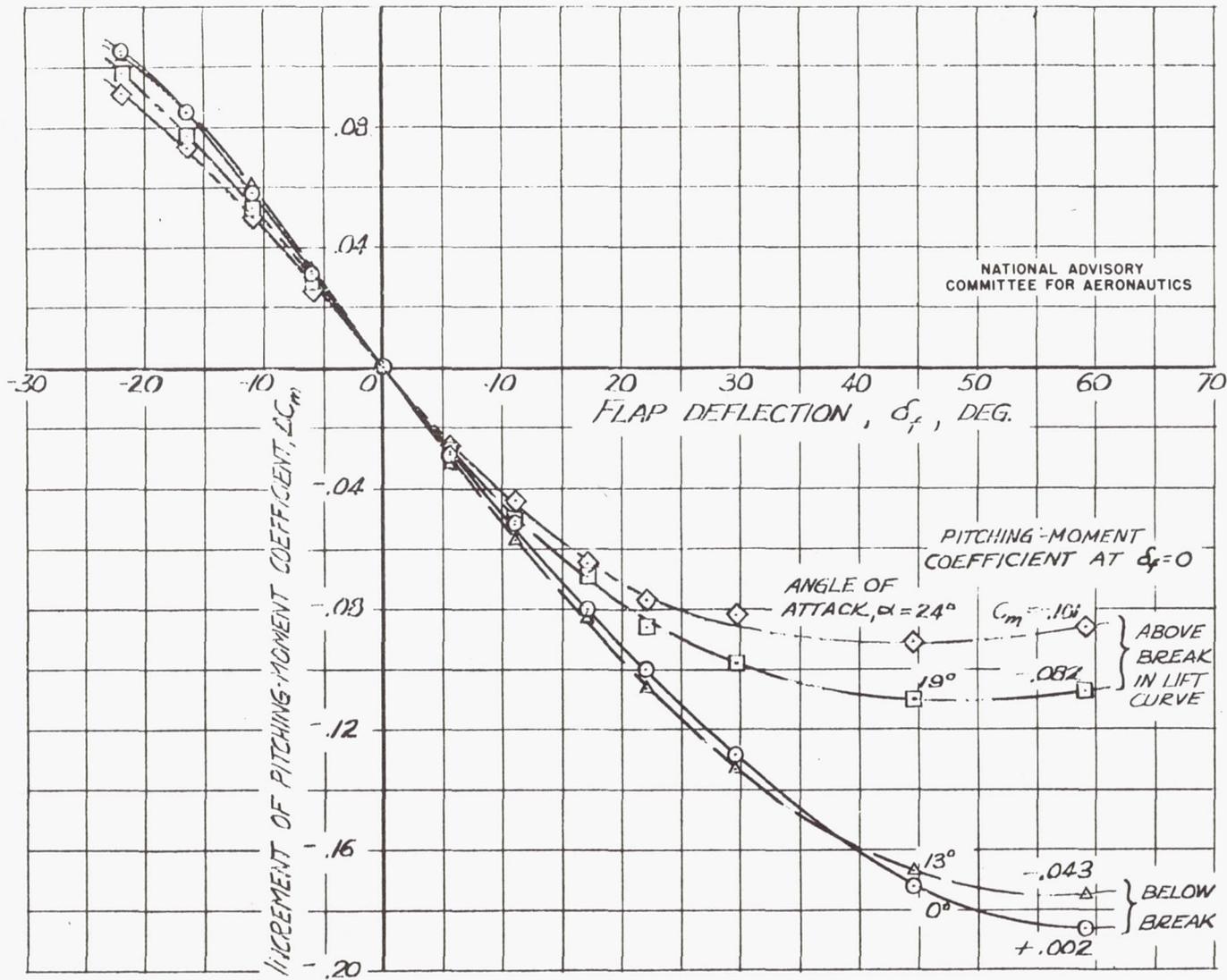
FIGURE 18.- INCREMENT OF PITCHING MOMENT COEFFICIENT DUE TO FLAP DEFLECTION AT CONSTANT ANGLE OF ATTACK.
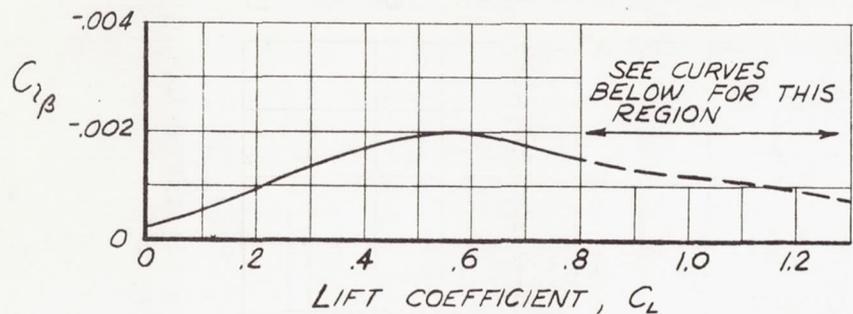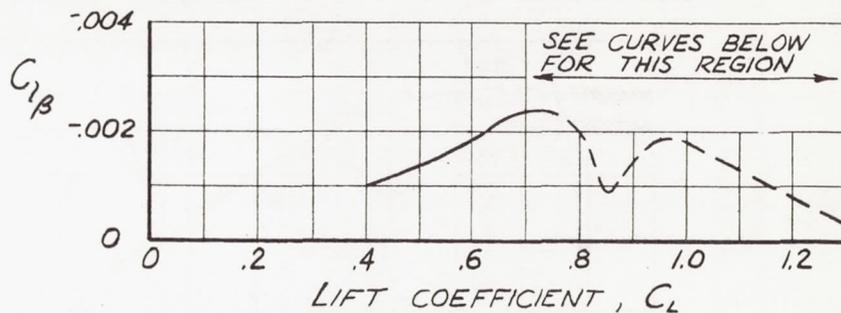
C_{l_β} | -.004 | -.002 | 0

SEE CURVES BELOW FOR THIS REGION

LIFT COEFFICIENT, C_L

(a) PLAIN WING, C_{l_β}

C_{l_β} | -.004 | -.002 | 0

SEE CURVES BELOW FOR THIS REGION

LIFT COEFFICIENT, C_L

(b) FLAPS DEFLECTED 44.5°, C_{l_β}

NATIONAL ADVISORY COMMITTEE
FOR AERONAUTICS

ROLLING-MOMENT COEFFICIENT, C_l | .02 | 0 | -.02 | -.04

C_L
1.20
.10
.92
1.02
.40
.80

ANGLE OF SIDESLIP, β, DEG.

(c) PLAIN WING, C_l vs β

ROLLING-MOMENT COEFFICIENT, C_l | .02 | 0 | -.02 | -.04

C_L
1.20
.40
1.00
.70
.85

ANGLE OF SIDESLIP, β, DEG.
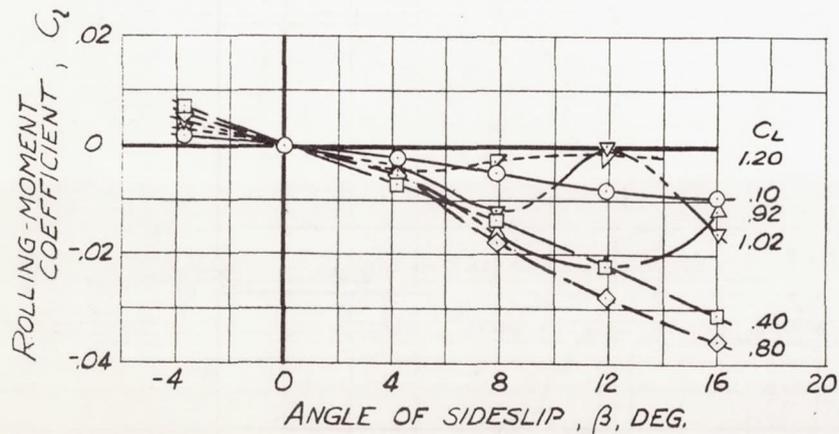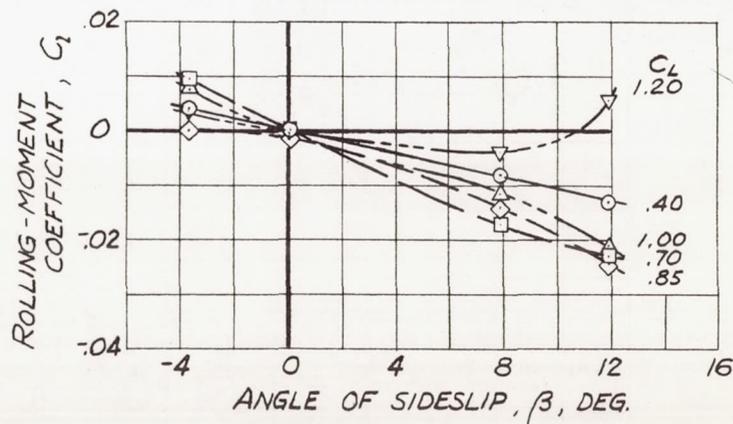
(d) FLAPS DEFLECTED 44.5°, C_l vs β

FIGURE 19.- LATERAL CHARACTERISTICS OF THE WING WITH AND WITHOUT FLAPS DEFLECTED.

Fig. 19

Fig. 20

(a) SUMMARY CURVES

NATIONAL ADVISORY COMMITTEE
FOR AERONAUTICS
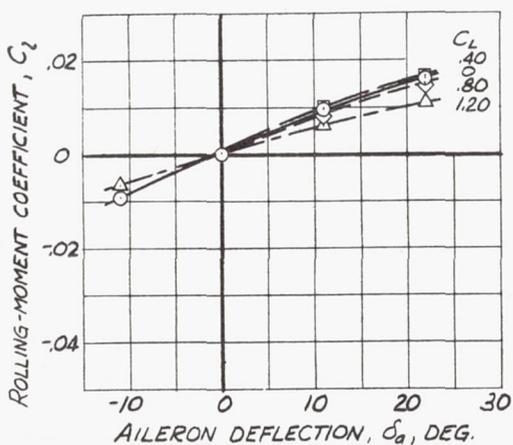
(b) RIGHT AILERON, $\beta = 0°$
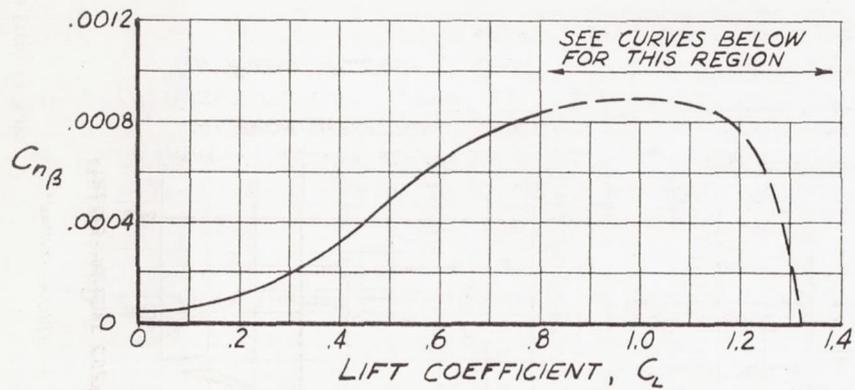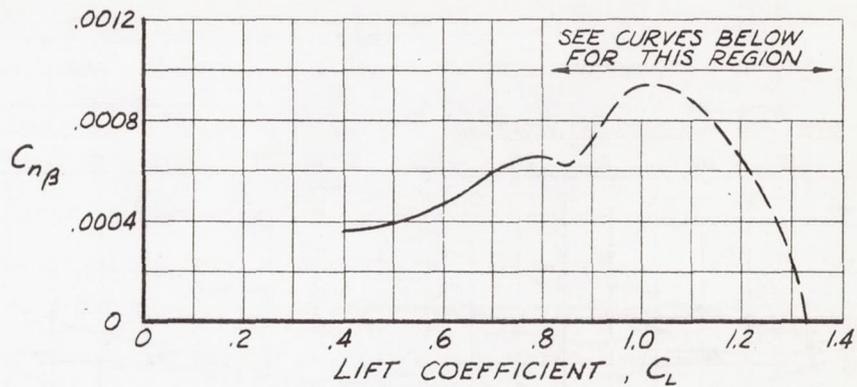
(c) RIGHT AILERON, $\beta = 11.9°$
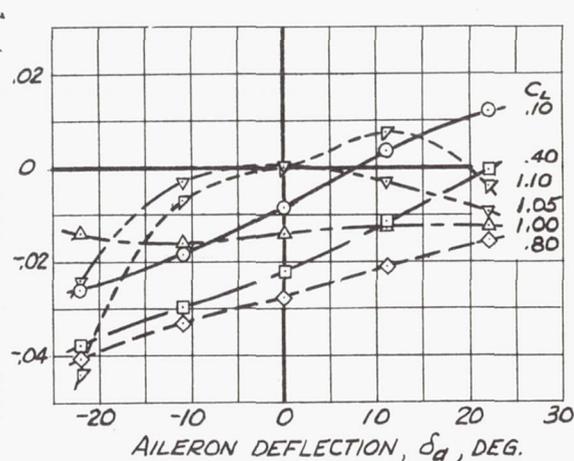
(d) LEFT AILERON, $\beta = 11.9°$

NOTE: AILERON ANGLE CONSIDERED POSITIVE FOR RIGHT STICK TRAVEL

FIGURE 20.— LATERAL CHARACTERISTICS OF WING WITH AILERON DEFLECTED.

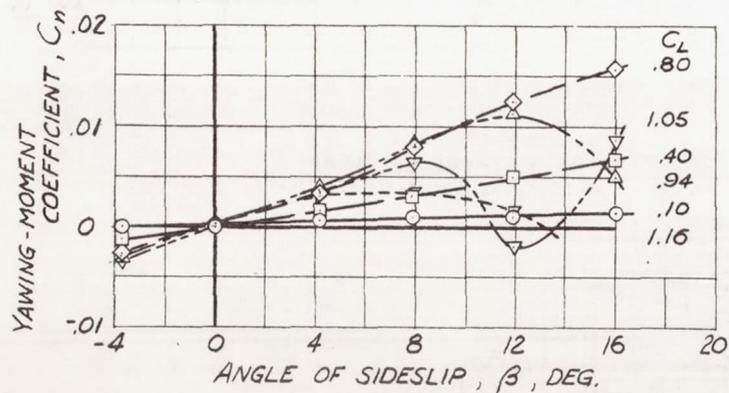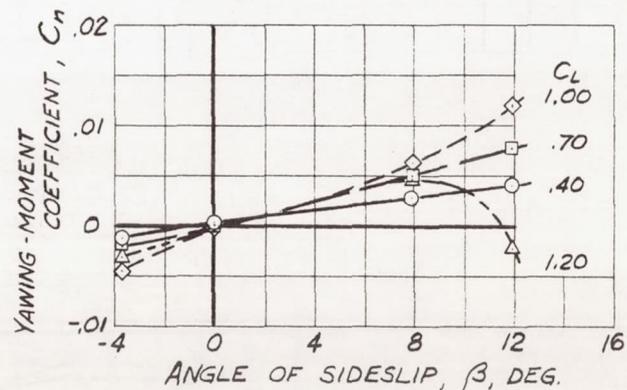(a) PLAIN WING, C_{n_β}

NATIONAL ADVISORY COMMITTEE
FOR AERONAUTICS
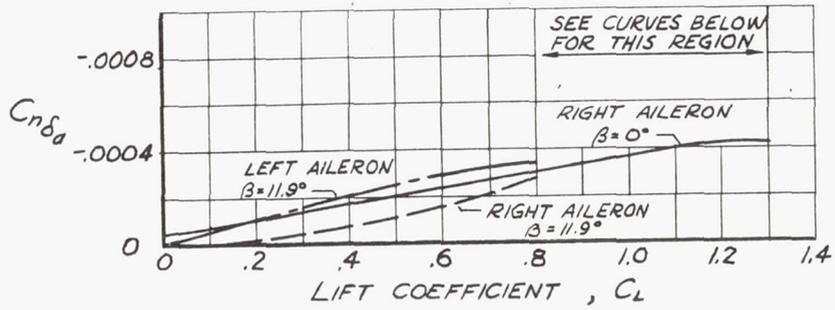
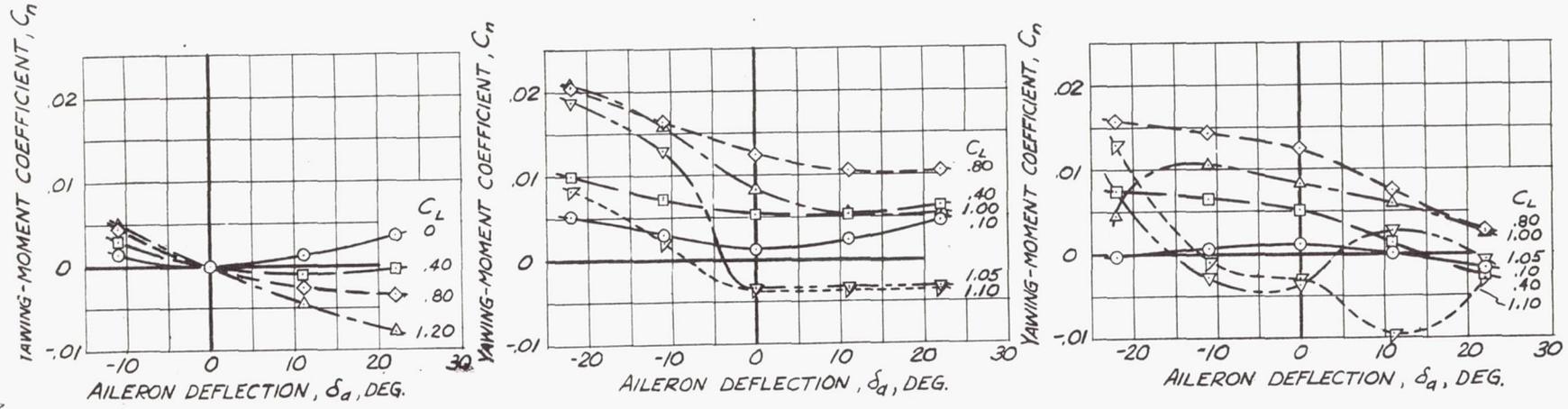(b) FLAPS DEFLECTED 44.5°, C_{n_β}

(c) PLAIN WING, C_n vs β

(d) FLAPS DEFLECTED 44.5°, C_n vs β

FIGURE 21.- DIRECTIONAL CHARACTERISTICS OF THE WING WITH AND WITHOUT FLAPS DEFLECTED.

Fig. 21

Fig. 22

(a) SUMMARY CURVES

(b) RIGHT AILERON , β=0°

(c) RIGHT AILERON , β=11.9°

(d) LEFT AILERON , β=11.9°

NOTE: AILERON ANGLE CONSIDERED POSITIVE FOR RIGHT STICK TRAVEL

FIGURE 22.- DIRECTIONAL CHARACTERISTICS OF THE WING WITH AILERONS DEFLECTED.